

## Editor comments:

Comments to the Author:

Two of the three original referees have looked again at the paper.

Both see it as usefully improved, but not without continuing flaws.

Referee 2 provides a detailed list of recommended further changes.

I see some of these as particularly sensible -- e.g. the current length/lack of focus of Section 5. I have looked at the paper in some detail myself and have set out some detailed comments below.

Please can you provide a revised version of the paper which addresses the comments of Referee 2 and my own comments, plus responses (particularly in cases where you have chosen not to make recommended changes).

I hope that I will then be able to accept the paper without further consultation with Referee 2 -- but I would need to consult if I felt that Referee 2's comments had not been properly considered.

## Detailed comments:

-----  
**p1 l13 and later:** You use the term 'synoptic situation' -- what do you mean exactly, i.e. what are the identifying characteristics of this synoptic situation?

### reply:

By 'synoptic situation' we meant the overall atmospheric large-scale wind and temperature distributions, which contribute to the water vapour drop (phase 2). Indeed, the term is not well chosen and we replace it by ``dynamical state'' and explain (at first occurrence in the revised text) what is meant.

The identifying characteristics of the dynamical state are the low cold point temperatures in the tropics and the corresponding increased upwelling.

Note that for a more detailed analysis of cause-effect relationships, our simulation results are not sufficient, because our free running simulation (RC1) is only one possible realisation and we cannot exclude, whether the result is by chance. All we can say is that there are strong indications that the SST cannot be ruled out as contributor.

-----  
**p2 l15:** Did Solomon et al (2010) really say that the water vapour anomalies HAD CAUSED a reduction in the surface warming trend. My understanding is that they said that the radiative forcing due to the water vapour anomalies had a magnitude that was 25% of the change in radiative forcing due to greenhouse gas trends over a similar period. This is not the same thing!

### reply:

Cited from the abstract of Solomon (2010):

``Stratospheric water vapor concentrations decreased by about 10% after the year 2000. Here we show that this ACTED TO SLOW the rate of increase in global surface temperature over 2000-2009 by about 25% compared to that which would have occurred due only to carbon dioxide and other greenhouse gases. ``

In order to avoid further confusion, we cite this literally in the revised manuscript.

-----  
**p7 l7:** 'Without observed SSTs die millennium drop ... cannot be simulated at all' -- 'die' should be 'the'.

More seriously -- the logical implication of this is that 'observed SSTs are necessary to simulate the millennium drop'. But in your nudged run you may have included SSTs (which allows you to make the statement above) but they may have had

no significance at all -- the TTL temperature anomalies may have arisen without the SSTs. I'm not convinced that you have shown any evidence that the SST anomalies are essential for the TTL temperature anomalies associated with the water vapour drop.

**reply:**

``Die'' is now corrected.

Our argumentation, why the observed SSTs contribute to the millennium drop is that RC2 (modelled SSTs compared to observed SSTs in RC1, both free running simulations) does not simulate the drop, especially phase 2, at all. RC1, however, captures some elements of it. Therefore, we concluded that the SSTs at least contribute to the characteristics of the drop.

Nevertheless, we see, that our conclusion is in so far not fully convincing, as RC1 might only by chance simulate features of the drop, because it is ``free running''. More realisations of RC1 with the same model setup would be necessary to prove/strengthen our conclusion.

We weaken our statement in the revised manuscript and add a sentence to the outlook to state the further need for sensitivity modelling studies to prove (or not) the importance of SSTs for the drop phase 2.

-----  
**p11 l25:** The comment above applies here too.

**reply:**

For the drop phase 2, we agree as we state above.

For the drop phase 1, however, we have shown that preceding El Nino/La Nina and their influence on upwelling contribute to the large declines observed. Here, we do not rely on one free running representation, but we have analysed more than one sudden decline. Note, however, that we completely agree that in principle other causes might also trigger such declines as well, although we did not find any in our data.

We clarify this explicitly in the revised manuscript.

-----  
**p13 l9:** 'Whilst this part is understood ... the connection between temperature and moisture is far more complicated.

' -- the two parts of the sentence seem to be in slight contradiction -- what exactly is the part of the temperature/moisture relation that is understood and what exactly is the part that is far more complicated.

**reply:**

What we meant with the 'part' that 'is understood' is written beginning at line 6, p 13 and refers to the processes that influences

the tropical tropopause temperature: ``The variability of tropopause temperature is dominated on an inter-annual period by modulations of ..El Nino, QBO..

Variations in ozone amplify the impact of those drivers.

In our analysis this relationship seems to be sufficient to show the connection between large water vapour drops (phase 1), QBO phases and preceding El Ninos.'

Generally, cold point temperature and moisture are positively correlated.

But we agree, that the ``connection between temperature and moisture is far more complicated'' is misleading. What we wanted to say is, that the moisture variability can be influenced also by other processes (transport, supersaturated regions, cirrus, overshooting ice during convective events).

All these processes were neglected in our analysis. We reformulate this sentence

to clarify it.

-----

**Referee #3:**

The authors have substantially altered their original submission, and have satisfactorily addressed most of my original issues. I have a few remaining general comments, plus a few more technical questions.

**General Comments:**

**A.** It might be worth noting somewhere that the La Nina event which started in fall of 1998 (after the unusually strong El Nino in 97/98) was quite unusual in its duration and intensity. Strong La Nina conditions were present for two straight years (both the winter of 98/99 and 99/00 were strong La Nina). It did not fully decay until the summer of 2001, though it was largely gone by spring of 2000 (when the drop started). One location I certainly recommend mentioning this is at the beginning of section 5. Section 5 seems poorly motivated at present.

**reply:**

We include the information on the extra-ordinary La Nina event in the revised Section 5.

According to our motivation of section 5:

In this section we analyse other sudden stratospheric water vapour declines (phase 1) and try to understand, what they have in common with the phase 1 of the ``millennium drop''. In particular, we examine the role of preceding El Nino/La Nina events, QBO phase and upwelling anomalies.

To clarify this in the revised manuscript we add this at the beginning of revised Section 5.

-----  
**B.** For clarity and reproducibility, can the markers for ENSO events be the same in all figures?

**reply:**

We unified the markers for the ENSO events. They represent the maximum of the corresponding SST anomaly as stated in Fig. 8a.

-----  
Figures 11-15 use the date of the respective temperature drops, while in earlier figures it isn't clear what exact metric is being used (the captions just say 'strong El Nino events'). Can the same 'temperature drop' metric be used in earlier figures as well? Alternately, the date of the 'temperature drop' can be added to the earlier figures.

**reply:**

In Figure 3 (and only there) we analyse the timing of the `` water vapour drop'', of which we define the ``date'' as the ``onset'', i.e., the largest value before the decline. (Note that this is different from the publication by Fueglistaler (2012), his Figure 9, who defines the ``drop date'' by the MINIMUM in water vapour). This is clarified in the revised caption of Figure 3.

The El Nino events in Figures 7, 8, 9, and 10 are (in the revised manuscript) indicated by vertical lines at the maximum of the corresponding SST anomaly (see Figure 8). To clarify this, we expand the Figure captions accordingly.

In Figures 11 to 15 in contrast, we use the temperature anomaly maximum at 80 hPa for overlaying (in time) the temporal development of similar events (in order

to analyse their common characteristics). This is also clarified in the revision.

In the first set of figures (Figs. 7 - 10), we use the El Nino occurrence to look for subsequent sudden declines (drop phase 1), whereas in the second set of figures (Figs. 11 - 15) we look from a different perspective, namely from the stratospheric temperature anomaly, in order to assess the underlying processes.

As we show in the text and Fig. 16 there is a non-constant delay between El Nino occurrence and onset of the subsequent decline. Thus, we could not use the El Nino ``dates'' in Figures 11 - 15. On the other hand, the decline onsets could indeed be added (as additional lines) to Figures 7 - 10 (or a subset), but this would require that we refer in Figure captions 7 - 10 to definitions and analyses that occur only later in the text.

Therefore, we are a bit hesitating to do so, because it does not improve the readability of our manuscript, but we want to leave the final decision on this to the editor.

-----  
**C.** I still find section 5 to be somewhat long-winded and repetitive. It is likely that the length of this section could be reduced (in both the number of figures shown and the text). Earlier sections are now much clearer than in the original draft.

**reply:**

We shorten Section 5 and move the figures 11-15 and 17 to the supplement.

-----  
**D.** The authors need to add a figure showing the evolution of zonal wind at 90hpa and 70hPa for each of the experiments and in the Singapore radiosonde. The authors argue that only the RC1SD captures the 90hPa QBO (which is clearly important for water vapor), but they never actually show this explicitly. If space is an issue, such a figure can be included in the supplemental material. This figure belongs in section 2, but should be referred to throughout the rest of the paper.

**reply:**

We added a figure with the zonal mean wind evolution (90 and 70 hPa) of our simulations in comparison with the Singapore radiosonde data. The figure is placed in the supplement. This figure is introduced in Section 2.

-----  
**Minor, technical comments:**

Page 1, line 5 'best reproduce' or 'most-closely reproduce' (currently 'best' on line 6 is misplaced)

**reply:**

corrected.

-----  
Page 1 line 11 'westerly' not 'western'.

**reply:**

corrected.

-----  
Also, it is really the transition to easterlies from the westerlies that lead to transition from relative downwelling (and warmth) to tropical upwelling and rapidly cooling cold point.

**reply:**

We agree and reformulated this passage in the abstract.

-----  
The last line of the abstract is more mechanistically correct. This is more evident for the drops shown in figure 15 other than the 97/98 one.

**reply:** Is this a question? Unfortunately, we do not get the point here.

-----  
Page 1 line 17 'simulated' to 'simulate'

corrected.

-----  
Page 2 , line 7 '.. content was observed ...'

corrected

-----  
Page 2, line 30 the comma is not needed

corrected.

-----  
Page 6 line 1 shouldn't this be 'the duration of phase 2', not phase 1?

**reply:**

Phase 1 is correct, because Figure 3 only shows the characteristics of the decline in water vapour, i.e. phase 1. We will add this information in the Figure captions of Fig. 3 and Fig. A1.

-----  
Page 6, line 23 it might be helpful to note that you will quantify this effect later in the paper (in figure 6 and at the top of page 7).

**reply:**

We placed a sentence at line 23, where we refer to the end of the Section for further explanation of the origin of these underestimated water vapour anomaly.

-----  
Page 6, line 30 end of line 'Because of this difference, RC2 shows neither the water vapor decline nor the long period...

corrected.

-----  
Page 7, line 7, die -> the

**reply:**

corrected.

-----  
Page 7, line 9 I suggest revising this sentence to refer to cold temperature as opposed to increased upwelling. While it is obvious that the two are linked as discussed in the next section, at this point in the manuscript the authors' have focused on cold temperature and not increased upwelling.

**reply:**

Thank you for this hint. We revised this sentence.

-----

Page 10, line 9 to 11 I found this sentence very confusing. Please rewrite.

**reply:**

Indeed this sentences is confusing. In order to shorten Section 5 as suggested this sentence is eliminated.

-----

Page 12, line 16 to 18 I found this sentence very confusing. Please rewrite. I think what is meant is that phase 1 is quite robustly associated with El Nino followed by La Nina, but phase 2 is associated more with synoptic variability that has little (or nothing) to do with the previous ENSO event,

**reply:**

Thank you for your reformulation. We corrected the sentence in the revised manuscript.

-----

Figure 9: I found it hard to follow the discussion of this figure. Can you make the x-axis tick marks that corresponds to 1980, 1985, 1990 1995, 2000, 2005, and 2010 bold or longer as in other figures? It is impossible to tell which tick mark corresponds to these years. Also, please add the El Nino label already shown in figure 9b in Figure 9a as well. A white font color should work well. It may also be clearer if the vertical lines for each event were longer, and reached up to 100hPa instead of ending at 300hPa. The x-axis tick marks in figure 8 are also unclear.

**reply:**

We improve the figures 8ab and 9ab accordingly.

-----

Page 12, line 19 what is meant by 'both'

**reply:**

corrected.

-----

Figure 3 I suggest putting titles for each column, e.g. 'model' and 'satellite'

**reply:**

At the last stage of the revision, we have been asked to include the more important titles (drop size, etc.), as they are now. Before that, we had ``model'' and ``observations''. We feel that including both now will make the figure too busy, and the information is in the caption anyway.

-----

Figure 16, 17 I suggest adding to the title 'El Nino' in red. Also, it might be helpful to add lines corresponding to the QBO near 80hPa to these figures in a third color.

**reply:**

We added the (normalised) QBO data into Fig.16. The Fig. 17 is moved to the supplement. In Fig. 17 we did not include the QBO anomaly, because the information is already shown in the Fig.S7 (former Fig. 15).

-----

Supplemental material S2 through S6: I don't understand why the 86/87, 98/99, and

09/10 events are included here, as they are already included in the 'drops with ENSO' category.

**reply:**

These figures were included because of a suggestion by Referee #2, who asked for sudden declines without preceding El Nino/La Nina events. The figures show that in years, in which no strong El Nino/La Nina event preceded in the year before, the water vapour drops (phase 1) are of smaller amplitude.

Note however, that here the ``events'' (86/87, 98/99, and 09/10) refer to the water vapour decline onsets and not to the El Ninos. This is clarified in the revised manuscript / supplement.



# The millennium water vapour drop in chemistry-climate model simulations

S. Brinkop<sup>1</sup>, M. Dameris<sup>1</sup>, P. Jöckel<sup>1</sup>, H. Garny<sup>1</sup>, S. Lossow<sup>2</sup>, and G. Stiller<sup>2</sup>

<sup>1</sup>Deutsches Zentrum für Luft- und Raumfahrt (DLR), Institut für Physik der Atmosphäre, Oberpfaffenhofen, Germany

<sup>2</sup>Karlsruher Institut für Technologie (KIT), Institut für Meteorologie und Klimaforschung, Karlsruhe, Germany

*Correspondence to:* S. Brinkop (sabine.brinkop@dlr.de)

**Abstract.** This study investigates the abrupt and severe water vapour decline in the stratosphere beginning in year 2000 (the “millennium water vapour drop”) and other similarly strong stratospheric water vapour reductions by means of various simulations with the state-of-the-art Chemistry-Climate Model (CCM) EMAC (ECHAM/MESSy Atmospheric Chemistry Model). The model simulations differ with respect to the prescribed sea surface temperatures (SSTs) and whether nudging is applied or not. The CCM EMAC is able to most-closely reproduce the signature and pattern of the water vapour drop in agreement with those derived from satellite observations best, if the model is nudged. Model results confirm that this extraordinary water vapour decline is in particular obvious in the tropical lower stratosphere and is related to a large decrease in cold point temperature. The drop signal propagates under dilution to the higher stratosphere and to the poles via the Brewer-Dobson circulation (BDC). We found that the driving forces for this significant decline in water vapour mixing ratios are tropical sea surface temperature (SST) changes due to a coincidence with a preceding strong El Niño–Southern Oscillation event (1997/98) followed by a strong La Niña event (1999/2000) and supported by the prevailing western change of the westerly to the easterly phase of the equatorial stratospheric quasi-biennial oscillation (QBO) at the drop onset in 2000. Correct (observed) SSTs are important to trigger the strong decline in water vapour and also, There are indications, that at least partly, for SSTs contribute to the long period of low water vapour values from 2001 to 2006. For this period, the specific synoptic situation dynamical state of the atmosphere (overall atmospheric large-scale wind and temperature distribution) is important as well, as it causes the observed persistent low cold point temperatures. These are induced by a period of increased upwelling, which, however, has no corresponding pronounced signature in SSTs anomalies in the tropics. Our free-running simulations do not capture the drop as observed, because a) the cold point temperature has a low bias and thus the water vapour variability is reduced and b) because they do not simulate the appropriate synoptic situations simulate the appropriate dynamical state. Large negative water vapour declines are also found in other years, and seem to be a feature, which can be found after strong combined El Niño/La Niña events, if the QBO west phase during La Niña changes to the east phase.

## 1 Introduction

Since the early 1980’s balloon-borne stratospheric water vapour measurements (e.g., Hurst et al., 2011) and climate models have predicted a continuous increase in stratospheric water vapour concentrations (SPARC CCMVal, 2010; Stenke and

Grewe, 2005; [SPARC CCMVal, 2010](#); Gettelman et al., 2010). Satellite measurements have not yet observed such an increase (UARS/MLS, UARS HALOE, and SAGE II instruments; see for instance Solomon et al., 2010; Hartmann et al., 2013). However, if we look from the late 1980s/early 1990s to now, we actually find a decreasing trend from merged satellite observations in the lower stratosphere (see Hegglin et al., 2014). The explanation of this has become a large scientific challenge and a lot of discussion persists, if Boulder balloon observations are representative, or if there is an issue in the satellite data merging.

An increase in stratospheric water vapour with time is expected as a net result of global warming as predicted for the 21st century by coupled CCMs (Gettelman et al., 2010). However, multi-year data sets show significant fluctuations on different time scales, which make it difficult to assess robust trends (Hegglin et al., 2014).

In the year 2000, an extraordinary sudden drop of stratospheric water vapour content ~~has been was~~ observed (e.g., Randel et al., 2006; Fueglistaler et al., 2005; Rosenlof and Reid, 2008; Maycock et al., 2014), which brought again into focus that temperature fluctuations have a large potential to significantly impact the amount of water vapour in the stratosphere. The strong and widely noticed water vapour drop in the year 2000 is particularly remarkable due to the fact, that it is followed by a 5 year period of low stratospheric humidity. Randel and colleagues showed that the tropical tropopause temperatures remain noticeably lower than normal after the decline due to an increase in tropical upwelling. The ~~coldest lowest~~ temperatures after the drop lie over the western tropical Pacific/Indonesia region and Africa during all seasons of the year, but are not a major feature in the Caribbean or the mid-Pacific (Rosenlof and Reid, 2008). ~~These negative water vapour anomalies after 2001 lead to a reduction in the~~ [Solomon et al. \(2010\) found that stratospheric water vapour concentrations decreased by about 10% after the year 2000. They showed that “this acted to slow the rate of increase in global surface temperature warming trend of over 2000-2009 by about 25\(Solomon et al., 2010\)-% compared to that which would have occurred due only to carbon dioxide and other greenhouse gases.”](#)

Since water vapour is the most prominent greenhouse gas, and therefore is an important contributor to variations and trends in climate, it is necessary to better understand its large variability. Stratospheric water vapour variations are connected with temperature changes in the tropical region, especially with the cold-point temperature (Randel et al., 2004; Fueglistaler, 2013). Changes of stratospheric water vapour levels ranging from inter-annual to decadal time scales are less well understood, in particular the contribution of processes involved. Well-known and understood is the “tape-recorder” effect (Mote et al., 1996) describing the annual cycle of the tropical stratospheric water vapour amount in accordance with the seasonally varying cold point temperature (e.g., Fueglistaler et al., 2005). Moreover, variations of the tropopause temperatures are clearly related to tropical upwelling, the equatorial quasi-biennial oscillation of stratospheric zonal winds (QBO), and the El Niño–Southern Oscillation (ENSO) as for example discussed by Randel et al. (2004). Recent analyses of the observed stratospheric water vapour record show that many of the variations on time scales of one to several years can be linked to changes in tropical tropopause temperatures, but some discrepancies still exist (e.g., Schoeberl et al., 2012; Fueglistaler et al., 2013). Randel and Jensen (2013) state that the water vapour fluctuations observed by satellite instruments over the last 20 years are not adequately reproduced by “free-running” Chemistry-Climate Models (CCMs), although those were forced by observed sea-surface temperatures (SSTs) and concentrations of greenhouse gases and ozone depleting substances were prescribed. Randel and Jensen point out ~~r~~ that current CCMs are not able to reconstruct the severe water vapour drop after the beginning of year

2000. Therefore, they conclude that important components of internal variability might be missing or at least under-represented in the model systems, especially in the tropical tropopause layer (TTL). Similar investigations summarise that it is still unclear whether the inability to simulate the observed trends is due to the large uncertainties in the observed stratospheric water vapour and tropical tropopause temperatures (e.g., Wang et al., 2012), inaccuracies in the CCMs, or whether the models miss relevant mechanisms (see Chapter 4 in WMO, 2014).

Here we present results of a set of 4 simulations with different model setups with the state-of-the-art chemistry-climate model (CCM) EMAC (ECHAM/MESSy Atmospheric Chemistry model), indicating that it is possible to retrace the observed water vapour fluctuations in the stratosphere (including the millennium drop). In the following section the CCM EMAC is briefly described, the investigated model simulations and the used observational data sets are presented. The millennium water vapour drop as represented in one of the model simulations is compared to observations in Sect. 3. To clarify, which part of the millennium drop we refer to, we define two different phases of “the drop”: phase 1 is the short period of the steep decline between the drop onset, i.e., the water vapour maximum, and its subsequent minimum. Phase 2 is the period of low values between the minimum and the start of the recovery. In Sect. 4 all model simulations are compared with respect to their ability to represent the millennium drop. Sec. 5 provides an analysis of other large moisture anomalies in the lower stratosphere and their relation to preceding El Niño/La Niña events. An overall discussion of our findings is given in Sect. 6.

## 2 Method and data

### 2.1 Description of the model system

The ECHAM/MESSy Atmospheric Chemistry (EMAC) model is a numerical chemistry and climate simulation system that includes sub-models describing tropospheric and middle atmosphere processes and their interaction with oceans, land and human influences (Jöckel et al., 2010). It uses the second version of the Modular Earth Submodel System (MESSy2) to link multi-institutional computer codes. The core atmospheric model is the 5th generation European Centre Hamburg general circulation model (ECHAM5, Roeckner et al., 2006). For the present study we analysed EMAC (ECHAM5 version 5.3.02, MESSy version 2.50) in the T42L90MA-resolution, i.e. with a spherical truncation of T42 (corresponding to a quadratic Gaussian grid of approx. 2.8 by 2.8 ° in latitude and longitude) with 90 vertical hybrid pressure levels up to 0.01 hPa.

The multi-year simulations have been performed with the CCM EMAC in the framework of the ESCiMo project (Earth System Chemistry integrated Modelling, Jöckel et al., 2016). Within ESCiMo so-called reference (RC) simulations have been carried out, as defined by the IGAC/SPARC Chemistry-Climate Model Initiative (CCMI) and described in detail by Eyring and Lamarque (2012). The forcing of the transient reference simulations in either free-running (RC1; from 1960 to 2011) or in a nudged mode (RC1SD, RC1SDNT; from 1980 to 2012) are similar (“hindcast simulations”). They are taken from observations or empirical data, including anthropogenic and natural forcing based on changes in trace gases, solar variability and volcanic eruptions (see Table 1 for an overview). The sea surface temperatures (SSTs) and the sea ice concentrations (SICs) are from observations or reanalysis data (RC1: HadISST, RC1SD and RC1SDNT: ERA-interim). In the case of RC1SD the model prognostic variables (vorticity, divergence, the logarithm of the surface pressure, the temperature and additionally the mean

temperature (wave number zero in spectral space)) are nudged by Newtonian relaxation towards ERA-Interim reanalysis data. RC1SDNT is nudged similarly with the exception that the mean temperature is NOT nudged. The transient forecast reference simulation RC2 (from 1960 to 2100) is a future projection that follows the IPCC scenario RCP 6.0 and a specified scenario of the development of ozone depleting substances (halogen scenario A1; WMO, 2007). It also considers solar variability in the past and future (for details see Jöckel et al., 2016). Because of potential discontinuities between the observed and simulated data record, RC2 uses SSTs and SICs derived from a coupled climate model simulation (with an interactive ocean, HadGEM2, RCP6.0 scenario; Johns et al., 2011) for the entire period. In the following analysis we confine the data of the RC2 simulation from 1960 to 2040.

The internal generation of a QBO is a feature of the L90MA setup of EMAC (Giorgetta et al., 2002). Therefore, in all simulations a QBO is internally generated. Nevertheless, the zonal winds near the equator are nudged towards a zonal mean field with a Gaussian profile in the latitudinal direction and with a relaxation time scale of 58 days in our simulations to get the correct phasing of the observed QBO (Jöckel et al., 2016). The nudging is applied in the altitude range between 10-90 hPa, with full nudging weights (i.e., 1.0) from 20-50 hPa, levelling off to 0.3 (0.2) at the upper (lower) edge of the nudging region. Full nudging is utilised between 7°S-7°N latitudes. As ~~will be shown in the results,~~ can be seen in (Fig. S1, supplement), this does not necessarily mean, that the QBO is equal in all simulations! The nudged model simulations (RC1SD, RC1SDN) better represent the observed zonal mean wind component in amplitude and absolute values compared to the observed winds (Singapore radiosonde). RC1 and RC2 simulate the QBO at 90 hPa only poorly, but capture to some extend the variability at 70 hPa.

## 2.2 Observational data sets

For comparison with our EMAC simulation with specified dynamics RC1SD (nudged mode), we use (i) the water vapour data from combined HALOE (Halogen Occultation Experiment) and MLS satellite measurements as described in Randel and Jensen (2013), (ii) a merged data set from seven limb-viewing satellite instruments, which were compiled into a long-term record (Hegglin et al., 2014) and (iii) a combination of satellite observations performed by HALOE and MIPAS (Michelson Interferometer for Passive Atmospheric Sounding) instruments (Russell et al., 1993; Fischer et al., 2008). For more details see the Appendices A1-A3.

With the data set (iii) we performed a novel analysis on several zonal mean characteristics of phase 1 of the millennium drop as a function of altitude and latitude (Appendix A4). Based on derived start and end dates of this phase 1 (i.e., from its maximum to its minimum anomaly), we calculate the length (duration) of phase 1, the start date (months since January 2000), and the size (amplitude). The same analysis was applied to the simulated stratospheric water vapour of RC1SD. This analysis is based solely on running annual means and does not imply an inter-comparison of periods before (2000) with periods after (2001) the decline, in contrast to previous studies (Randel et al., 2006; Maycock et al., 2014).

### 3 The millennium water vapour drop

This study is motivated by a chart which is shown in Fig. 1 (the original figure was published by Randel and Jensen, 2013): The near-global lower stratospheric water vapour anomalies were derived from multi-year satellite measurements (1992–2012) from HALOE and Aura/MLS at the 83 hPa pressure level (approximately 17 km altitude). The measurements impressively indicate inter-annual fluctuations of up to 15 % (about 0.5 ppmv) from the 20 year mean mixing ratio. There are clear signs of the QBO over the full time period. The figure highlights the severe water vapour drop (approximately  $-0.7$  ppmv) in the year 2000.

The HALOE data (see Fig. 1) show a step like change from an enhanced water vapour period before the drop (1993–2000) into a phase with reduced water vapour. The recovery from this phase (our phase 2) with prevailing negative anomalies starts in 2007. The RC1SD simulation (nudged, including mean temperature nudging) closely reproduces the water vapour fluctuations as observed. The timing of relative minimum and maximum water vapour values is reproduced very well. Evidently the model underestimates the strength of the inter-annual fluctuations (only about 0.3 ppmv instead of 0.5 ppmv) compared to the combined HALOE/Aura-MLS satellite data. The amplitude of the severe drop (phase 1) in 2000 is by about 0.12 ppmv smaller than in the combined HALOE/Aura-MLS satellite data, yet the period with lower than normal water vapour (phase 2) is captured well. The deviation of the RC1SD simulation results from the merged data set by (Hegglin et al., (2014, )) (see Fig. 1) is even smaller. RC1SD and the merged data set agree in particular with respect to a) the start of the recovery phase after the drop, which starts earlier as in the HALOE data, b) the amplitude of the drop, and c) the lower water vapour anomalies in the period before the drop. The merged data set consists of individual short satellite records, merged with the simulated water vapour from a chemistry-climate model, which was nudged to observed meteorology. For the lower stratosphere this record of water vapour mixing ratios largely follows tropical tropopause temperatures. This might be the reason why the RC1SD and the merged data set are in better agreement.

Fig. 2 (also corresponding to Fig. 2 of Randel & Jensen, 2013) moreover shows that the cold point temperature anomalies of RC1SD follow those of the radiosonde data. This can be expected, due to the nudging of EMAC towards ERA-Interim data.

There are expectations that the water vapour drop in observations exhibits different characteristics at different latitudes and altitudes with respect to the start date, the drop size (amplitude) and the length (duration) of the anomaly. For example, Urban et al. (2014) ~~show~~showed that in the tropics the significant reduction of water vapour started in the altitude range from 16.5 to 18.5 km (375–425 K) in early 2000, whereas between 25 and 30 km (625–825 K) it began in late 2001. Moreover, they ~~demonstrate~~demonstrated that the drop was more pronounced in the lower tropical stratosphere than in the middle stratosphere, i.e.  $-1.3$  and  $-0.6$  ppmv, respectively. The minimum water vapour mixing ratios were found in the lower stratosphere about one year, in the middle stratosphere almost two years after the onset of the drop.

Here, we perform a novel, comprehensive analysis to quantify the characteristics of the water vapour drop (phase 1): a) the amplitude (drop size), b) the duration of the drop (drop length), and c) the onset of the drop (drop date). The results are shown in Fig. 3 as a function of latitude and altitude for both, the combined HALOE/MIPAS data set (Schiederdecker, 2015) and for the RC1SD simulation. The details of the methodology are described in Appendix A4.

The amplitude (drop size) of the drop maximises in the tropical lower stratosphere consistently in observations and the RC1SD simulation (Fig. 3, top). However, the amplitude in the tropics is larger in the observations. Towards higher latitudes and altitudes up to about 20 hPa the drop amplitude typically decreases. Above this level some increase in the drop amplitude can be observed that goes along with a stronger QBO variability. It is unclear if the drop amplitude here can be unambiguously attributed to the millennium drop or simply reflects natural QBO variability or a combination of both.

A similar pattern can be seen for the start date of the millennium drop (Fig. 3, middle). Up to 40 hPa the drop occurs in most cases during the year 2000. Above 30 hPa there is a clear shift to dates in 2002 and 2003, again mostly controlled by QBO variability. The stronger branch of the Brewer–Dobson circulation on the Northern Hemisphere is clearly visible in the earlier start dates of the drop compared to the Southern Hemisphere.

The duration of phase 1 is the less consistent quantity (Fig. 3, bottom). Values typically range from 6 months (inherent from the approach) to about 20 months. In the simulation the length is in the order of 9 months in the lowermost tropical stratosphere. The observations exhibit here longer drops related to the larger drop amplitudes.

In conclusion, Fig. 3 nicely reflects that the cold point tropopause anomaly reduces water vapour and that this signal propagates into the upper stratosphere and, a bit asymmetrically due to the different branches of the Brewer-Dobson circulation, further towards the poles.

#### 4 The millennium water vapour drop in other ESCiMo simulations

In the last [Section](#), we showed that the millennium water vapour drop is reasonably well reproduced by the RC1SD simulation with nudged mean temperature. In the following we investigate whether also the other simulations RC1SDNT, RC1 and RC2 (see Table 1) are capable to simulate the variability of lower stratospheric water vapour, and in particular the drop in year 2000.

The RC1SDNT (without mean temperature nudging) simulated water vapour anomaly time series amplitude is by a factor of about 1/3 too small (Fig. 4). Additionally, the period of low water vapour anomaly (phase 2) has a too high minimum. However, the tropical cold point temperature anomalies (Fig. 5) are in better agreement with RC1SD. Since RC1SD and RC1SDNT differ only with respect to the nudging of the global mean temperature, the RC1SD simulation implies a bias correction and RC1SDNT is affected by this bias. Therefore, the smaller water vapour anomaly amplitude in RC1SDNT is likely caused by a tropical cold point temperature of 189.4 K, which is biased low compared to that of RC1SD (192.1 K) within the 1992–2012 period. Contemporary CCMs show a large spread of about 10 K in simulating cold point tropopause temperatures (Gettelman et al., 2009). This corresponds to the likewise wide spread of simulated ozone at the tropopause level and to differently simulated tropopause altitudes. Since the cold point temperature strongly affects stratospheric water vapour, we conclude that in order to correctly simulate water vapour anomalies in time and amplitude, it is not sufficient to reproduce the temperature anomaly. The mean cold point temperature must be simulated correctly as well. The explanation for this is the non-linear dependence of water vapour on temperature as described by the Clausius-Clapeyron equation.

The magnitude of inter-annual variability in water vapour in the tropical lower stratosphere is overall far lower in the free-running simulation RC1 (Fig. 4). We will discuss and quantify this at the end of this section. However, a decrease in water vapour around the year 2000 is found also in RC1. The strength of the drop (phase 1) is underestimated by a factor of 2. The minimum period (phase 2) is visible but the minimum is far too high. Compared to RC1SDNT, the free-running RC1 simulation does not simulate the observed ~~synoptic-situation~~atmospheric dynamical state. Yet, this seems also to be important for reproducing the observed water vapour variability, in particular the millennium drop. This is consistent with results of Garfinkel et al. (2013b), who showed with model simulations forced by observed SSTs only, that SSTs alone cannot explain the timing and the subsequent recovery of the millennium drop.

The main difference between the RC2 and RC1 simulation is that RC2 uses simulated instead of observed SSTs. Because of this difference, ~~RC2 is therefore neither showing~~shows neither the water vapour decline, nor the long period with low water vapour values after 2000. Accordingly, no low cold point temperature anomalies are visible in Fig. 5.

The effect of the correct cold point temperature on the saturation water vapour value is also demonstrated for the RC1 simulation (Fig. 6). We took the temperature variability of RC1 as shown in Fig. 5, but used the actual cold point mean temperature as simulated in RC1SD. Thus, we shifted the cold point temperature anomalies. Then we calculated the corresponding saturation moisture over ice for RC1SD (just for comparison), for RC1 (original simulation) and for RC1shifted (shifted cold point temperature anomaly). The results show that a corrected absolute cold-point temperature of RC1 (i.e., RC1shifted) is expected to improve the representation of phase 2 of the drop.

We conclude: (1) Without observed SSTs ~~die the~~ millennium drop (phase 1 ~~and 2~~) cannot be simulated ~~at all~~. There are indications, that observed SSTs contribute to phase 2, also. (2) The specific ~~synoptic-situation~~atmospheric dynamical state as simulated by RC1SD and RC1SDNT seems to be important for the representation of the millennium drop (phase 2). Note, that the period of ~~increased upwelling~~low cold point temperature after 2001 has no ~~corresponding distinct~~ signature in observed tropical SSTs. (3) The correct cold point temperature is necessary to simulate the correct minimum of low water vapour values (phase 2) and the amplitude of the drop (phase 1).

## 5 Other large negative moisture anomalies (phase 1) in the lower stratosphere and their relation to preceding El Niño/La Niña events

~~The millennium drop in water vapour 2000/01~~ In this section we analyse other sudden stratospheric water vapour declines (phase 1) ~~after the strong 1997/98 El Nio event is followed by an unusual long time period of relatively low water vapour values~~ (phase 2) (Fig. ~~and try to understand, what they have in common with the phase 1~~). ~~Since Solomon et al. (2010) found that these anomalous low water vapour values in the lower stratosphere caused a reduced trend in global surface temperatures over the years 2000–2009 by about 25, we wonder, if this millennium drop is unique or if we can expect that such a decline is a more or less typical feature of stratospheric water vapour variability? Is there a relation to preceding of the “millennium drop”. In particular, we examine the role of preceding~~ El Niño/La Niña ~~events? The El Nio Southern Oscillation is an ocean–atmosphere~~



~~feedback that occurs every 2–5 and propagates throughout the troposphere into the lower stratosphere. Therefore events, related upwelling anomalies and the QBO.~~

It is well understood that El Niño/La Niña events have the potential to ~~couple the surface temperature with the stratosphere affect stratospheric variability through SST anomalies~~ (Scaife et al., 2003; Randel et al., 2009; Calvo et al., 2010; Garfinkel et al., 2013a). ~~The La Nina event which started in fall of 1998 (after the unusually strong El Niño in 97/98) was quite unusual in its duration and intensity. Strong La Niña conditions were present for two straight years (both the winters of 98/99 and 99/00 were strong La Niña). It did not fully decay until the summer of 2001, though it was largely gone by spring of 2000 (when the drop started). In the tropical lower stratosphere the QBO is the dominant dynamic feature (Rosenlof and Reid, 2008; Dessler et al., 2014) that contributes to the extraordinary temperature fluctuation in the tropical tropopause region. It appears as a reversal of the tropical zonal wind direction with a mean period of about 28 months (ranging from 22 to 34 months) and is a primarily wave-driven stratospheric phenomenon.~~

We have analysed the time evolution of water vapour anomalies for the RC1SD and RC1 simulations at 80 hPa (Fig. 7) for the full time period available for the respective simulations. In the RC1 simulation we found 5 and in the RC1SD simulation 3 relatively large water vapour declines (phase 1) marked by a red asterisk, which are comparable to the millennium drop amplitude in the respective simulation. An additional asterisk marks a smaller water vapour decline after the 1986/87 El Niño in RC1SD, which additionally was examined.

Because the amplitudes in the RC1 simulation are generally smaller than in RC1SD, we define a “large decline” in the simulations differently: RC1SD: decline  $> 0.5$  ppmv, and for RC1: decline  $> 0.2$  ppmv.

The thresholds have been only used to simplify the search of decline events with preceding ENSO events. Thus, the result of event identification counting is independent of the selected values. We could have also started with the ENSO index and searched for decline events after La Niña events. The result is the same.

Although there are 2 other large water vapour declines in the RC1SD simulation starting 1994 and 1996, we neglect this time period, because the eruption of Mt. Pinatubo (1991) had a significant impact on temperature and water vapour in our simulations (Löffler et al., 2015). Likewise, we cannot exclude, that the eruption of Mt. Chichon in 1982, although less strong than the eruption of Mt. Pinatubo had an influence on the results.

The dominant effect of El Niño/La Niña events on the tropical surface temperatures (including land and sea surface temperatures) are clearly visible in Fig. 8a in all simulations. The data derived from the RC1 simulation indicate strong temperature signals related to the El Niño and La Niña episodes (1: 1969/70, 2: 1973/74, 3: 1982/83, 4: 1986/87, 5: 1997/98, 6: 2009/10). The RC1SD simulation only covers El Niño and La Niña events from no 3 to no 6, but the surface temperatures are similar to RC1. ~~The 1997/98 El Nio event (5) was unusually strong compared to former events, with a tropical surface temperature amplitude of about 0.7, similar for both RC1 and RC1SD. Case no 4 shows a two year lasting El Nio starting as weak in 1986 and becoming 1987/88 a moderate event followed by a strong La Nia. The~~

The SSTs for the RC2 simulation were taken from a coupled ocean–atmosphere simulation of the HadGEM-model, and the tropical surface temperatures are generally lower than in observations (Fig. 8b). However, the simulated surface temperature



represent similar fluctuations (in magnitude) as observed, but originating in different periods of time and often with longer time duration.

~~In order to understand the origin of large water vapour declines, we analysed the corresponding development and incidence of two important components of natural variability influencing the temperature in the TTL: the El Niño/La Niña events and the QBO. The QBO appears as a reversal of the tropical zonal wind direction with a mean period of about 28 months (ranging from 22 to 34 months) and is a primarily wave-driven stratospheric phenomenon. In the tropical lower stratosphere the QBO is the dominant dynamic feature.~~

As mentioned above (Sect. 2), in all four EMAC simulations the QBO is nudged to zonal mean winds with respect to the amplitude and phase. Therefore the signature of the QBO in the temperature anomaly (Fig. 9b, RC1 as representative for all simulations) propagating downwards to the TTL is present in all ~~three~~ EMAC simulations (for the RC1SD simulation see Fig. ~~S1-S2~~ in the supplement). Although the QBO nudging setup is equal in all simulations presented, the resulting winds are not the same in RC1SD, RC1, and RC2. The QBO nudging does not force a one-by-one representation of the nudged data by the model, the model still develops its own dynamical state. Note that the QBO at roughly 90 hPa is key for the temperature signal affecting water vapour, i.e., at an altitude, where the QBO nudging strength is already reduced and therefore relies on signal propagation. Only for RC1SD (and RC1SDNT), where divergence and vorticity and the logarithm of the surface pressure are nudged, too, the wind profiles are close to those of ERA-interim (Fig. S1, supplement). The RC1 and RC2 simulations, however, show a smaller amplitude and the QBO is less visible at 90 hPa.

~~It is well-known (Rosenlof and Reid, 2008, Dessler et al., 2014) that the QBO phase contributes to the extraordinary temperature fluctuation in the tropical tropopause region around year 2000 due to an unusual long QBO phase: strong east winds in the equatorial lower stratosphere (around 30) were persistently detected for nearly two years (2000/01); the downward propagation of the zero-wind line (change from east to west wind direction) stopped for one year (from mid-2000 to mid-2001) at about 40.~~

Around a strong El Niño event (black vertical lines, Fig. 9b) we find a positive moisture (Fig. 9a) and temperature anomaly throughout the troposphere up to about 100 hPa and subsequent moistening of the lower stratosphere. This result is consistent with the findings of Dessler et al. (2014), who showed by regression analysis that stratospheric entry values of water vapour increase with tropospheric temperature. El Niño as an important driver of the inter-annual variability is captured in the tropical tropospheric temperature regressor. In contrast, the effect of La Niña events to increase stratospheric water vapour as discussed by Garfinkel et al. (2013a) is not captured with the tropospheric temperature regressor, but with the BDC (Brewer-Dobson circulation) regressor.

In Fig. 9, in a narrow layer between 100 and 50 hPa (marked with dashed black lines) a negative temperature anomaly occurs, except for the 1982/83 El Niño, where a positive QBO phase with warming probably masks this feature. For the 1997/98 and the 2009/10 El Niño the cooling is not pronounced, but also visible.

Positive and negative temperature anomalies in the narrow layer are related to a large part by changes in upwelling (Fig. 10), which directly modifies the tropopause temperature through lifting of air masses. Additionally, a positive upwelling anomaly (cooling) is accompanied by a negative ozone anomaly (cooling, not shown). For this reason upwelling anomaly and ozone

anomaly are anti-correlated with a Pearson's correlation coefficient of about  $r = -0.56$  at 70 hPa for both, RC1 and RC1SD (Table 2, see Appendix B for the formula of the Pearson's correlation coefficient). Tropical upwelling is calculated from the model results in terms of the residual vertical velocity  $w^*$  as introduced in the transformed Eulerian mean (TEM) equations (e.g. Holton, 2004, his equation 10.16b) for the tropics ( $20^\circ\text{S} - 20^\circ\text{N}$ ). As expected temperature and large-scale upwelling are also strongly anti-correlated with a Pearson's correlation coefficient  $r = -0.7$  (70 hPa) for RC1SD (RC1:  $r = -0.58$ ) (Table 2). Likewise temperature and QBO are positively correlated with  $r = 0.5$  (RC1) ( $r = 0.4$  for RC1SD) at 70 hPa. The correlation coefficient decreases at lower altitudes, because the effect of the QBO on temperature decreases.

In the TTL positive temperature anomalies always result in positive water vapour anomalies propagating upward into the stratosphere (Fig. 9). This is independent of a heating and moistening of the tropical troposphere during El Niños and occurs also under La Niña conditions. Because El Niño (La Niña) conditions lead to an increase (decrease) in upwelling (Fig. 9) a cooling (warming) of the TTL region can often be found (El Niños 1,2,4,5,6, La Niñas: 2,4,5,6). A moistening can occur in cases, where the mature phase of an El Niño is over and positive TTL anomalies appear. This is consistent with the results of Garfinkel et al. (2013a) who also find a moistening of the stratosphere after La Niña events. TTL temperature anomalies are an indicator of the regional dynamical properties (Mote et al., 1996; Randel et al., 2004). The traveling time for water vapour anomalies in the lower stratosphere calculated from the maximum correlation between temperature at 100 hPa and water vapour at 82 hPa is about 2 months (Rosenlof and Reid, 2008; Schoeberl et al., 2008).

We find a similar result only for RC1SD, but RC1 and RC2 exhibit the maximum correlation for lag = 0. Accordingly, the correlation between temperature and moisture at 70 hPa is stronger in RC1 ( $r = 0.8$ ) than in RC1SD ( $r = 0.4$ ). Consistently, upwelling is smallest in the RC1SD and largest in the RC1 simulation leading to a faster transport of water vapour through the TTL in RC1. Because nudging basically affects the whole momentum budget (e.g., resolved wave amplitudes, which largely drive upwelling, are nudged), it is not surprising that upwelling is different in the free running compared to the nudged simulation.

~~We use this connection to analyse the conditions under which large temperature drops occur, in order to understand the origin of large water vapour drops. In doing so, we disregard other processes that may contribute to the water vapour distribution and its variability in the TTL such as convective overshooting and large-scale water vapour transports, ice supersaturated regions and cirrus development.~~

Every El Niño event is generally accompanied by a strong positive upwelling anomaly (Fig. 10) followed by a period with reduced upwelling and thus positive temperature anomalies in the TTL. Many of these positive temperature anomalies mark the onset of strong drops in temperature and water vapour. Note the double maximum in the temperature anomaly after the 1972/73 (no 2) El Niño (Fig. 9b), which is related to the reduced upwelling in (Fig. 10-10). This confirms that upwelling plays the other important role in generating temperature anomalies around 100–60 hPa beside the QBO, directly through adiabatic cooling.

Although the SSTs of the RC1SD and RC1 simulation are similar, the period with a positive upwelling anomaly after the year 2001, leading to the observed low tropopause temperatures and low water vapour values in the lower stratosphere (Randel et al., 2006) is not adequately simulated in the RC1 simulation. ~~Interestingly after 2001, where tropical SSTs only exhibit~~

~~a small but long-lasting positive anomaly in both, RC1 and RC1SD, upwelling already shows a positive anomaly, stronger in RC1SD than in RC1.~~

If a strong El Niño plus La Niña event is typically followed by a large temperature/water vapour drop we might expect that typical conditions exist that favour these large variations. We performed an episode analysis for the previously selected 4 (RC1SD) and 5 (RC1) strong El Niño events, followed by a La Niña event (Fig. 8) and strong declines in water vapour, respectively, to emphasise the conditions that favour these large variations. Additionally, 4 smaller declines in water vapour of simulation RC1SD, where no ENSO event preceded, were selected and analysed. The results are presented in the supplement, together with the analysis of the RC1 simulation. Here we focus on the RC1SD simulation. The onset of the individual temperature declines at 80 hPa (Fig. 11, and supplement Figs. S3-S13) is placed at month 0, so that the periods before the drop and afterwards can be consistently analysed. In the figures, the period of the drop is marked by two vertical lines and the word “drop”. We selected the start of the temperature drop (rather than the drop in water vapour), where temperature is at its maximum, for the definition of the corresponding event, because QBO, upwelling and ozone have a direct effect on temperature. Water vapour anomalies follow temperature anomalies directly or with a time lag.

~~The onset of the millennium water vapour drop (Fig. 12, green dashed line) is phase shifted by 3 to 4 months and the 2009/10 water vapour drop about 2 months after the temperature maximum of the corresponding decline (Fig. 11). For the other declines in RC1SD and all declines in RC1, we find no time lag.~~

All onsets of the temperature drops of RC1SD ~~and RC1~~ are associated with a minimum in the large-scale upwelling anomaly (Fig. 13), accompanied by a maximum in ozone anomaly (Fig. 14) ~~and for RC1SD only, and~~ a west-phase of the QBO (Fig. 15). Accordingly, the minima of the drops show maxima in upwelling, minima in ozone and an east-phase of the QBO (for RC1SD only).

~~RC1 does not show the transition from west QBO to east QBO phase at the 80 level as a typical feature, because the QBO phases do not propagate down as far into the TTL as in RC1SD. Therefore, the contribution of the QBO phase to the drop is less for RC1.~~

Generally, the correlation between temperature anomaly and QBO anomaly is smaller in RC1 than in RC1SD for the 90 level compared to 70 (Table 2). This points to a different coincidence of upwelling and QBO in RC1, which might partly explain, why the anomalies in temperature and hence water vapour at TTL level are smaller in RC1.

The analysis of small declines of the RC1SD simulation (we placed the figures in the supplement, Fig. S2–Fig. S6) confirms our results. Small declines are not necessarily accompanied by the changing west to east phase anomaly of the QBO. A clear negative anomaly in upwelling (at the onset in phase 1) only exists for one decline. However, the amplitudes of the upwelling anomalies are smaller than the respective amplitudes for the large declines (Fig. 13).

The 11). Furthermore, the time evolution of the upwelling anomaly is strongly correlated with SST anomalies during El Niño and La Niña periods (El Niño region 3.4, Figs. 16 and 17 11 and S13 for RC1) except for the 1982/83 (no 3) El Niño event, which had its maximum already before the maximum of surface temperature was reached. However, for the whole simulation period in RC1SD upwelling anomalies and surface temperature anomalies in the tropics are only correlated with  $R = -0.4$ . ~~We conclude, that under~~ Under most El Niño/La Niña conditions the high/low SST anomalies have ~~the a~~ a dominant influence

on upwelling maxima and minima, and thus on the drop amplitude, ~~whereas~~. One exception is the water vapour decline after the 1982/83 El Niño, where the upwelling reached a maximum before the SST maximum. Moreover, under undisturbed SST conditions (without the influence of ENSO) the influence on upwelling is ~~smaller~~.

also smaller. The volcanic eruption of El Chichon in 1982 might have influenced water vapour variability (Löffler et al., 2015) during the 1982/83 El Niño. In the RC2 simulation large water vapour drops (phase 1) also occur, however, none of those show a clear relation with preceding ENSO events as analysed from the observations and from the other simulations. Furthermore, the correlation between upwelling and temperature (Table 2) is weaker in RC2 (compared to the other simulations). The reason are the different horizontal SST patterns, which are not as those observed. This affects the dynamics, e.g., stratospheric winds and thus wave propagation.

## 10 6 Summary and discussion

We use results of 4 different simulations performed with the CCM EMAC to analyse the millennium drop in stratospheric water vapour. The simulations differ with respect to the prescribed SSTs and whether nudging is applied or not (see Table 1). We find, that a nudged setup (RC1SD, including nudging of the global mean temperature) performs best compared to observations. A nudged setup excluding the mean temperature from nudging (RC1SDNT) also reproduces the millennium drop, however, with a smaller amplitude and a little too high water vapour values during the drop phase 2. This is solely related to the cold point temperature bias, because this is the only difference between RC1SD and RC1SDNT. The free-running RC1 simulation with observed SSTs grossly underestimates the drop, but can capture some elements of it, and the free running simulation with simulated SSTs (RC2) shows no drop at all. The analysed gradual degradation of the drop signal from RC1SD(NT) over RC1 to RC2 is further augmented by the difference in the QBO signal between the different simulations.

Our first conclusion is that the correct SSTs are important to trigger the drop (i.e., phase 1) and also, at least partly, for the period of low values in phase 2. However, the simulation of some of the characteristics of the millennium drop (phase 2) in RC1 does not give full confidence that the SSTs contribute significantly to the drop phase 2. The drop phase 2 might only be simulated by chance. Here, more realisations with the model setup of this “free running” simulation RC1 are necessary to confirm our suggestions. Second, the specific ~~synoptic situation~~ atmospheric dynamical state as simulated by RC1SD and RC1SDNT contributes to the characteristics of the millennium drop. This is especially true for phase 2, a period of increased upwelling after 2001, which has no corresponding pronounced signature in SSTs anomalies in the tropics. Finally, the correct absolute cold point temperature is necessary to simulate the correct minimum of low water vapour values (phase 2) and thus the amplitude of the drop (phase 1). The millennium drop of stratospheric water vapour of RC1SD in phase 1 is correlated with a strong negative tropical SST fluctuation from La Niña 1999/2000 (after an unusual strong positive tropical SST anomaly from El Niño 1997/98) with reduced upwelling at the onset of the decline and a positive phase of the QBO changing to the negative phase and stronger upwelling.

We also analysed the time series of water vapour anomalies in order to understand if there are similarities in the processes leading to large amplitudes in water vapour anomaly. In the RC1SD simulation strong drops in temperature and water vapour

at the tropopause (phase 1) and above can also be found after other El Niño events (e.g. 1982/83 and 2009/10) followed by a La Niña, when conditions comparable to the millennium drop occur: Reduced upwelling due to a La Niña event in coincidence with a west phase of the QBO (warming) followed by an increase in upwelling in connection with the east phase of the QBO (cooling). The reduced upwelling induces a positive ozone anomaly (warming) and vice versa.

5 In the RC1 simulation we also find large amplitudes in water vapour at the tropopause (phase 1) after ENSO events. However, the QBO anomalies are often not in phase with the temperature or water vapour decline. This affects the timing of declines displayed in Fig. 5, which is slightly different compared to RC1SD. In RC1 the temperature variability seems to be dominated more by upwelling, which is in absolute terms, also larger in RC1 than in RC1SD (~~Fig. 13~~Figs. S5-S7). This is at least not in contradiction to Dessler et al. (2014), who found that the BDC provides the largest part to the water vapour variability in the  
10 lower stratosphere. Nevertheless, from our nudged simulation RC1SD, which is more in accordance with ERA-Interim, we find the coincidence of reduced upwelling and QBO west phase anomaly changing to east in connection with the large declines (Fig. ~~13~~S3 and Fig. ~~15~~S5). In principle it might be, that other causes also trigger such declines as well, although we did not find it in our data.

During periods of strong surface forcing of a successive El Niño/La Niña event, the trend in the upwelling anomaly is often  
15 (but not always) strongly correlated to the SSTs in the El Niño 3.4 region (Figs. ~~16 and 17~~11 and Fig. S13). This connection was already stated by Calvo et al. (2010), and Deckert and Dameris (2008). Thus, ~~after an ENSO the potential for a large water vapour decline declines~~ (phase 1) ~~is increased, however it remains open, if a period with low water vapour values follows~~ (~~phase are quite robustly associated with strong El Niño followed by La Niña, but phase 2~~), ~~because the conditions for its appearance can be different as for the~~ is associated more with the dynamical state of the atmosphere and not with the previous ENSO event. The analysis of the detailed characteristics of the dynamical state in phase ~~1-~~  
20 2 in RC1SD, and RC1 is beyond the scope of the paper.

Tropical upwelling, that strongly controls temperature in the tropopause layer, is influenced ~~both~~ by the ENSO (see e.g. Calvo et al., 2010). We find that in the free-running simulation RC1 the QBO does not propagate downward far enough into the tropopause region. Furthermore, the relation of tropical SSTs/ENSO to upwelling is stronger in RC1 compared to the nudged simulation.

25 This raises the question, whether there are processes or forcing, which are missing or underrepresented in the RC1 and the RC2 simulations. Because SSTs are prescribed from similar observations, RC1SD and RC1 differ mainly with respect to the nudging (of temperature, vorticity, divergence, the logarithm of surface pressure), and the temperatures of land surfaces, which are not prescribed, but can evolve interactively. RC2 uses simulated SSTs, which are colder than those used for RC1. Therefore RC2 can be expected to show different results at least for the time evolution.

30 So far it is not clear, how many of the processes of the obtained cause and effect relationship are insufficiently described or parameterised. More investigations are needed to clarify, whether an inaccurate representation of these processes and ~~for~~ feedback mechanisms in EMAC is responsible, or if it is a matter of model resolution that leads to the disagreement regarding the strength of year-to-year fluctuations of water vapour and temperature. Moreover, a general problem of “free running” models is, that the cold point is slightly too high (Gettelman et al., 2009) and therefore a little too cold compared to observations,  
35 which already leads to a reduced variability in absolute humidity.

Looking at the now 22 year long global water vapour record constructed on satellite-instrument measurements, there is another severe water vapour drop of similar size apparent after 2011 (Urban et al., 2014). Once longer records of global measurements become available in the future, it might turn out that such significant stratospheric water vapour fluctuations occur regularly. Natural changes that affect the stratospheric water vapour content are modified by climate change itself, may impact future climate. This demonstrates that robust climate predictions need realistic fluctuations of SSTs and an adequate representation of the QBO to reproduce the observed stratospheric water vapour fluctuations. Obviously severe changes can have a “memory” effect, impacting climate change on a decadal time scale (Solomon et al., 2010).

The variability of tropopause temperatures is dominated on an inter-annual period by modulations of the El Niño–Southern Oscillation, the tropical upwelling, and the stratospheric QBO. Variations in ozone amplify the impact of those drivers. In our analysis this relationship seems to be sufficient to show the connection between large water vapour drops, QBO phases, and preceding El Niños. While ~~this part is these processes are~~ understood (Randel et al., 2006, 2009; Fueglistaler and Haynes, 2005; Jones et al., 2011; Urban et al., 2012; Fueglistaler et al., 2013; Randel and Jensen, 2013), the ~~connection between temperature and moisture is far more complicated.~~ moisture variability can also be influenced by horizontal transport, supersaturated regions, cirrus, and overshooting ice during convective events. All these processes were neglected in our analysis.

From Urban et al., (2014) we know that a period exists, where the variability of lower stratospheric water vapour is uncorrelated to the mean zonal temperature (2008–2011). The reason is so far unknown. Here, we omitted to analyse this period, because it is beyond the scope of this paper.

We further neglected in our analysis any possible changes in the transport of water vapour into the TTL, and the presence of supersaturated regions or cirrus clouds in the TTL. Since temperature and water vapour are non-linearly dependent, a monthly mean temperature does not give any information about the actual frequency distribution of saturation values of water vapour. In our simulations, the actual water vapour values are generally lower than the saturation values. It points to a lack of certain processes important for the budget of water vapour in the lower stratosphere (for instance convective overshooting). This is a topic of further research.

## Appendix A: Millennium drop characteristics

### 25 A1 UARS/HALOE

HALOE was deployed on UARS (Upper Atmosphere Research Satellite) and performed measurements from September 1991 to November 2005. The measurements were based on the solar occultation technique. Absorption spectra were obtained in specific spectral bands in the wavelength range between 2.5 and 11  $\mu\text{m}$ . Typically 30 occultations per day were performed, generally at two distinct latitude bands in the opposite hemispheres, based on sunrise and sunset measurements. Within a month the observations covered roughly the latitude range between 60° S and 60° N. Water vapour results were retrieved from the 6.54 to 6.67  $\mu\text{m}$  spectral range, typically covering altitudes from about 10 to 85 km. For the analysis here we use data retrieved with version 19, that have been used extensively (e.g. Kley et al., 2000; Randel et al., 2006; Scherer et al., 2008; Hegglin et al., 2013).

## A2 Envisat/MIPAS

To fill some observational gaps that are inherent of the solar occultation technique employed by the HALOE instrument we also consider MIPAS limb observations of thermal emission. Those provided typically more than 1000 individual measurements per day, lasting from June 2002 to April 2012. MIPAS was carried by Envisat (Environmental Satellite) which used a sun-synchronous orbit with full latitudinal coverage on a daily basis. The measurements covered the spectral range between 4.1 and 14.6  $\mu\text{m}$ . Initially a spectral resolution of  $0.035\text{ cm}^{-1}$  (unapodised) was used, however after an instrument failure in March 2004 later observations had to be performed with a reduced resolution of  $0.0625\text{ cm}^{-1}$  (Fischer et al., 2008). Here we utilise data that have been retrieved with the IMK/IAA (Institut für Meteorologie und Klimaforschung in Karlsruhe, Germany/Instituto de Astrofísica de Andalucía in Granada, Spain) processor. Water vapour information is retrieved from several microwindows in the wavelength range between 7.09 and 12.57  $\mu\text{m}$  providing data from 10 km up to the lower mesosphere. For the observations with high spectral resolution retrieval version 20, for the low resolution time period version 220 is used. Detailed information on these data sets can be found in Schieferdecker (2015) and Hegglin et al. (2013).

## A3 Data set combination

The combination is based on monthly zonal mean time series from the individual data sets. In the overlap period a time-independent shift is determined that minimises the offset between the time series in a root mean square sense. This shift is derived for every altitude level and latitude bin considered and subsequently applied to the MIPAS time series. Applications of the combined HALOE-MIPAS time series can be found in Eichinger et al. (2014) or Schieferdecker et al. (2015).

## A4 Analysis approach

The basic data for the analysis presented in Fig. 3 are monthly zonal mean data covering the time period from July 1998 to December 2005. The HALOE-MIPAS data set is interpolated in time to fill a few gaps. The data are averaged over a latitude range of  $20^\circ$  using a  $10^\circ$  latitude grid. The rather wide average in latitude aims to handle some of the sparseness of the HALOE observations. For the simulations this would not be necessary but for reasons of compatibility and comparability the same handling is applied. In the vertical the data sets extend from 100 to about 7 hPa and are interpolated on a regular grid using 16 levels per pressure decade.

The analysis is performed separately for every pressure level and latitude bin using the steps listed below. Figure A1 shows an example.

In a first step we calculate a running average over one year. In Fig. A1 the averaged time series is given by the black line. Based on that time series we calculate in the next step the gradient in water vapour along every data point.

Subsequently we look for periods with sequences of at least six data points that have a negative gradient allowing one data point in-between to have a positive or zero gradient. Typically we find several of such periods, as seen in the example in Fig. A1. We only consider those periods that have started within a certain time interval. For 100 hPa this interval ranges from January 2000 to January 2004, as indicated by the red lines in Fig. A1. This is based on a priori knowledge. For higher altitudes

we adjust the start of the interval to the start date of the millennium drop at 100 hPa. At this altitude the drop is typically easiest to observe and we expect that higher up no earlier start dates occur.

To decide which of the periods represents the millennium drop we rely on two parameters, one, the absolute change in water vapour and, two, its overall gradient. These parameters are calculated for every period. Subsequently the periods are ranked according to these parameters with the largest absolute value gaining the highest rank. The ranks for a period are summed up and the period with the lowest sum is considered as the period that most likely represents the millennium drop. In the example shown in Fig. A1 the first period is chosen to represent the millennium drop as it exhibits both the largest decrease and the strongest negative gradient among the possible periods.

## Appendix B: Pearson's correlation coefficient

Pearson's correlation coefficient is determined by:

$$r = \frac{\sum_{i=1}^n (a_i - \bar{a})(b_i - \bar{b})}{\sqrt{\sum_{i=1}^n (a_i - \bar{a})^2} \sqrt{\sum_{i=1}^n (b_i - \bar{b})^2}} \quad (\text{B1})$$

a and b are the data sets to be correlated. n is the number of values per data set and  $\bar{a} = \frac{1}{n} \sum_{i=1}^n a_i$ .

*Author contributions.* S. Brinkop prepared the manuscript and analysed the model results. M. Dameris was involved in the discussion of the data analysis results and supported the writing of the manuscript. H. Garny calculated the residual circulation based on the model simulations. P. Jöckel performed the simulations with EMAC. G. Stiller provided the MIPAS data and participated in the discussion. S. Lossow performed the novel analysis of the water vapour drop characteristics with the HALOE/MIPAS and the model simulation data.

*Acknowledgements.* This work has been funded by the Deutsche Forschungsgemeinschaft (DFG) within the research unit Stratospheric Change and its Role for Climate Prediction (SHARP-FOR 1095). The presented investigations were carried out within the water vapour project SHARP-WV. The model simulations were performed within the DKRZ project ESCiMo (Earth System Chemistry integrated Modelling). The merged data set of stratospheric water vapour was kindly provided by M. Hegglin. We would like to thank the Deutsches Klimarechenzentrum (DKRZ) for providing computing time and support and Christoph Kiemle for valuable comments on the manuscript. We thank S. Fueglistaler, M. Schoeberl and an anonymous referee for valuable comments on the manuscript.

The article processing charges for this open-access publication were covered by a Research Centre of the Helmholtz Association.



## References

- Calvo, N., Garcia, R. R., Randel, W. J., and Marsh, D. R.: Dynamical mechanism for the increase in tropical upwelling in the lowermost tropical stratosphere during warm ENSO events, *J. Atmos. Sci.*, 67, 2331–2340, 2010.
- Deckert, R. and Dameris, M.: Higher tropical SSTs strengthen the tropical upwelling via deep convection, *Geophys. Res. Lett.*, 35, L10813, doi:10.1029/2008GL033719, 2008.
- Dessler, A.E., Schoeberl, M.R., Wang, T., Davis, S.M., Rosenlof, K.H., and Vernier, J.-P.: Variations of stratospheric water vapor over the past three decades, *J. Geophys. Res.*, 119, doi:10.1002/2014JD021712, 2014.
- Eichinger, R., Jöckel, P., and Lossow, S.: Simulation of the isotopic composition of stratospheric water vapour – Part 2: Investigation of HDO/H<sub>2</sub>O variations, *Atmos. Chem. Phys.*, 15, 7003–7015, doi:10.5194/acp-15-7003-2015, 2015.
- Eyring, V. and Lamarque, J.-F.: Global chemistry-climate modeling and evaluation, *EOS Trans. AGU*, 93, 539, doi:10.1029/2012EO510012, 2012.
- Fischer, H., Birk, M., Blom, C., Carli, B., Carlotti, M., von Clarmann, T., Delbouille, L., Dudhia, A., Ehhalt, D., Endemann, M., Flaud, J. M., Gessner, R., Kleinert, A., Koopman, R., Langen, J., López-Puertas, M., Mosner, P., Nett, H., Oelhaf, H., Perron, G., Remedios, J., Rindolfi, M., Stiller, G., and Zander, R.: MIPAS: an instrument for atmospheric and climate research, *Atmos. Chem. Phys.*, 8, 2151–2188, doi:10.5194/acp-8-2151-2008, 2008.
- Fueglistaler, S., Bonazzola, M., Haynes, P., and Peter, T.: Stratospheric water vapor predicted from the Lagrangian temperature history of air entering the stratosphere in the tropics, *J. Geophys. Res.*, 110, D08107, doi:10.1029/2004JD005516, 2005.
- Fueglistaler, S., Liu, Y. S., Flannaghan, T. J., Haynes, P. H., Dee, D. P., Read, W. J., Remsberg, E. E., Thomason, L. W., Hurst, D. F., Lanzante, J. R., and Bernath, P. F.: The relation between atmospheric humidity and temperature trends for stratospheric water, *J. Geophys. Res.*, 118, 1052–1074, doi:10.1002/jgrd.50157, 2013.
- Garfinkel, C. I., Hurwitz, M.M., Oman, L.D., and Waugh, D.W.: Contrasting Effects of Central Pacific and Eastern Pacific El Niño on Water Vapor, *Geophys. Res. Lett.*, 40, Stratospheric4115–4120, doi: 10.1002/grl.50677, 2013a.
- Garfinkel, C.I., Waugh, D. W., Oman, L.D., Wang, L., and Hurwitz, M.M.: Temperature trends in the tropical upper troposphere and lower stratosphere: connections with sea surface temperatures and implications for water vapor and ozone, *J. Geophys. Res., Atmospheres*, 118(17), 9658–9672, doi: 10.1002/jgrd.50772, 2013b.
- Gottelman, A., Birner, T., Eyring, V., Akiyoshi, H., Bekki, S., Brühl, C., Dameris, M., Kinnison, D. E., Lefevre, F., Lott, F., Mancini, E., Pitari, G., Plummer, D. A., Rozanov, E., Shibata, K., Stenke, A., Struthers, H., and Tian, W.: The Tropical Tropopause Layer 1960–2100, *Atmos. Chem. Phys.*, 9, 1621–1637, doi:10.5194/acp-9-1621-2009, 2009.
- Giorgetta, M. A., Manzini, E., and Roeckner, E.: Forcing of the quasi-biennial oscillation from a broad spectrum of atmospheric waves, *Geophys. Res. Lett.*, 29(8), doi:10.1029/2001GL014756, 2002.
- Hartmann, D. L., Klein Tank, A. M. G., Rusticucci, M., Alexander, L. V., Brönnimann, S., Charabi, Y., Dentener, F. J., Dlugokencky, E. J., Easterling, D. R., Kaplan, A., Soden, B. J., Thorne, P. W., Wild, M., and Zhai, P. M.: Observations: Atmosphere and Surface, in: *Climate Change 2013: The Physical Science Basis. Contribution of Working Group I to the Fifth Assessment Report of the Intergovernmental Panel on Climate Change*, edited by: Stocker, T. F., Qin, D., Plattner, G.-K., Tignor, M., Allen, S. K., Boschung, J., Nauels, A., Xia, Y., Bex, V., and Midgley, P. M., Cambridge University Press, Cambridge, UK, and New York, NY, USA, 2013.
- Hegglin, M. I., Tegtmeier, S., Anderson, J., Froidevaux, L., Fuller, R., Funke, B., Jones, A., Lingenfelter, G., Lumpe, J., Pendlebury, D., Remsberg, E., Rozanov, A., Toohey, M., Urban, J., von Clarmann, T., Walker, K. A., Wang, R., and Weigel, K.: SPARC Data Initia-

- tive: Comparison of water vapor climatologies from international satellite limb sounders, *J. Geophys. Res.-Atmos.*, 118, 11824–11846, doi:10.1002/jgrd.50752, 2013.
- Hegglin, M. I., Plummer, D. A., Shepherd, T. G., Scinocca, J. F., Anderson, J., Froidevaux, L., Funke, B., Hurst, D., Rozanov, A., Urban, J., von Clarmann, T., Walker, K. A., Wang, H. J., Tegtmeier, S., and Weigel, K.: Vertical structure of stratospheric water vapour trends derived from merged satellite data, *Nat. Geosci.*, 7, 768–776, 2014.
- Holton, J. R.: *An Introduction to Dynamic Meteorology*, International Geophysics Series, 4th edn., Academic Press, San Diego, New York, USA, 2004.
- Hurst, D. F., Oltmans, S. J., Vömel, H., Rosenlof, K. H., Davis, S. M., Ray, E. A., Hall, E. G., and Jordan, A. F.: Stratospheric water vapor trends over Boulder, Colorado: analysis of the 30 year boulder record, *J. Geophys. Res.*, 116, D02306, doi:10.1029/2010JD015065, 2011.
- 10 Jöckel, P., Kerkweg, A., Pozzer, A., Sander, R., Tost, H., Riede, H., Baumgaertner, A., Gromov, S., and Kern, B.: Development cycle 2 of the Modular Earth Submodel System (MESSy2), *Geosci. Model Dev.*, 3, 717–752, doi:10.5194/gmd-3-717-2010, 2010.
- Jöckel, P., Tost, H., Pozzer, A., Kunze, M., Kirner, O., Brinkop, S., Cai, D. S., Frank, F., Garny, H., Gottschaldt, K.-D., Graf, P., Grewe, V., Kern, B., Matthes, S., Mertens, M., Meul, S., Nützel, M., Oberländer-Hayn, S., Ruhnke, R., Runde, T., and Sander, R.: Earth System Chemistry Integrated Modelling (ESCiMo) with the Modular Earth Submodel System (MESSy, version 2.51), *Geosci. Model Dev.*, accepted 2016.
- 15 Jones, C. D., Hughes, J. K., Bellouin, N., Hardiman, S. C., Jones, G. S., Knight, J., Liddicoat, S., O'Connor, F. M., Andres, R. J., Bell, C., Boo, K.-O., Bozzo, A., Butchart, N., Cadule, P., Corbin, K. D., Doutriaux-Boucher, M., Friedlingstein, P., Gornall, J., Gray, L., Halloran, P. R., Hurtt, G., Ingram, W. J., Lamarque, J.-F., Law, R. M., Meinshausen, M., Osprey, S., Palin, E. J., Parsons Chini, L., Raddatz, T., Sanderson, M. G., Sellar, A. A., Schurer, A., Valdes, P., Wood, N., Woodward, S., Yoshioka, M., and Zerroukat, M.: The HadGEM2-ES implementation of CMIP5 centennial simulations, *Geosci. Model Dev.*, 4, 543–570, doi:10.5194/gmd-4-543-2011, 2011.
- Kley, D., Russell, J. M., and Philips, C.: *Stratospheric Processes and their Role in Climate (SPARC) – Assessment of Upper Tropospheric and Stratospheric Water Vapour*, SPARC Report 2, WMO/ICSU/IOC World Climate Research Programme, Geneva, Switzerland, 2000.
- Maycock, A. C., Joshi, M. M., Shine, K. P., Davis, S. M., and Rosenlof, K. H.: The potential impact of changes in lower stratospheric water vapour on stratospheric temperatures over the past 30 years, *Q. J. Roy. Meteor. Soc.*, 140, 2176–2185, doi:10.1002/qj.2287, 2014.
- 25 Mote, P. W., Rosenlof, K. H., Holton, J. R., Harwood, R. S., and Waters, J. W.: An atmospheric tape recorder: the imprint of tropical tropopause temperatures on stratospheric water vapor, *J. Geophys. Res.*, 101, 3989–4006, 1996.
- Randel, W. J. and Jensen, E. J.: Physical processes in the tropical tropopause layer and their roles in a changing climate, *Nat. Geosci.*, 6, 169–176, doi:10.1038/ngeo1733, 2013.
- Randel, W. J., Wu, F., Oltmans, S. J., Rosenlof, K., and Nedoluha, G.: Interannual changes of stratospheric water vapor and correlations with tropical tropopause temperatures, *J. Atmos. Sci.*, 61, 2133–2148, 2004.
- 30 Randel, W. J., Wu, F., Vömel, H., Nedoluha, G. E., and Forster, P.: Decreases in stratospheric water vapor after 2001: links to changes in the tropical tropopause and the Brewer–Dobson circulation, *J. Geophys. Res.*, 111, D12312, doi:10.1029/2005JD006744, 2006.
- Randel, W. J., Garcia, R. R., Calvo, N., and Marsh, D.: ENSO influence on zonal mean temperature and ozone in the tropical lower stratosphere, *Geophys. Res. Lett.*, 36, L15822, doi:10.1029/2009GL039343, 2009.
- 35 Roeckner, E., Brokopf, R., Esch, M., Giorgetta, M., Hagemann, S., Kornblüeh, L., Manzini, E., Schlese, U., and Schulzweida, U.: Sensitivity of simulated climate to horizontal and vertical resolution in the ECHAM5 atmosphere model, *J. Climate*, 19, 3771–3791, doi:10.1175/JCLI3824.1, 2006.

- Rosenlof, K. H. and Reid, G. C.: Trends in the temperature and water vapor content of the tropical lower stratosphere: sea surface connection, *J. Geophys. Res.*, 113, D06107, doi:10.1029/2007JD009109, 2008.
- Russell, J. M., Gordley, L. L., Park, J. H., Drayson, S. R., Hesketh, W. D., Cicerone, R. J., Tuck, A. F., Frederick, J. E., Harries, J. E., and Crutzen, P. J.: The halogen occultation experiment, *J. Geophys. Res.*, 98, 10777–10797, 1993.
- 5 Scaife, A. A., Butchart, N., Jackson, D.R., and Swinbank, R.: Can changes in ENSO activity help to explain increasing stratospheric water vapor? *Geophys. Res. Lett.*, 30, 1880, doi:10.1029/2003GL017591, 17.
- Scherer, M., Vömel, H., Fueglistaler, S., Oltmans, S. J., and Staehelin, J.: Trends and variability of midlatitude stratospheric water vapour deduced from the re-evaluated Boulder balloon series and HALOE, *Atmos. Chem. Phys.*, 8, 1391–1402, doi:10.5194/acp-8-1391-2008, 2008.
- 10 Schieferdecker, T.: Variabilität von Wasserdampf in der unteren und mittleren Stratosphäre auf der Basis von HALOE/UARS und MI-PAS/Envisat Beobachtungen, PhD thesis, Karlsruhe Institute of Technology, available at: <http://digbib.ubka.uni-karlsruhe.de/volltexte/1000046296>, last access: 22 June 2015.
- Schieferdecker, T., Lossow, S., Stiller, G. P., and von Clarmann, T.: Is there a solar signal in lower stratospheric water vapour?, *Atmos. Chem. Phys.*, 15, 9851–9863, doi:10.5194/acp-15-9851-2015, 2015.
- 15 Schoeberl, M. R., Dessler, A. E., and Wang, T.: Simulation of stratospheric water vapor and trends using three reanalyses, *Atmos. Chem. Phys.*, 12, 6475–6487, doi:10.5194/acp-12-6475-2012, 2012.
- Schoeberl M., Douglass, A., Stolarski, R., Pawson, S., Strahan, S., and Read, W.: Comparison of lower stratospheric tropical mean vertical velocities, *J. Geophys. Res. Atmos.*, 113, D24109, doi:10.1029/2008JD010221, 2008.
- Shepherd, T. G. and McLandress, C.: A robust mechanism for strengthening of the Brewer–Dobson circulation in response to climate change: critical-layer control of subtropical wave breaking, *J. Atmos. Sci.*, 68, 784–797, doi:10.1175/2010JAS3608.1, 2011.
- 20 Solomon, S., Rosenlof, K. H., Portmann, R. W., Daniel, J. S., Davis, S. M., Sanford, T. S., and Plattner, G.-K.: Contributions of stratospheric water vapor to decadal changes in the rate of global warming, *Science*, 327, 1219–1223, doi:10.1126/science.1182488, 2010.
- SPARC CCMVal (Stratospheric Processes And their Role in Climate): SPARC Report on the Evaluation of Chemistry-Climate Models, edited by: Eyring, V., Shepherd, T. G., and Waugh, D. W., SPARC Report No. 5, WCRP-132, WMO/TD-No. 1526, 478 pp., available at:
- 25 [http://www.atmosp.physics.utoronto.ca/SPARC/ccmval\\_final/index.php](http://www.atmosp.physics.utoronto.ca/SPARC/ccmval_final/index.php) (last access: 22 June 2015), 2010.
- Stenke, A. and Grewe, V.: Simulation of stratospheric water vapor trends: impact on stratospheric ozone chemistry, *Atmos. Chem. Phys.*, 5, 1257–1272, doi:10.5194/acp-5-1257-2005, 2005.
- Urban, J., Lossow, S., Stiller, G., and Read, W.: Another drop in water vapor, *EOS*, 95, 245–246, 2014.
- Wang, L., Zou, C.-Z., and Qian, H.: Constructions of stratospheric temperature data records from Stratospheric Sounding Units, *J. Climate*,
- 30 25, 2931–2946, doi:10.1175/JCLI-D-11-00350.1, 2012.
- WMO (World Meteorological Organization), Scientific Assessment of Ozone Depletion: 2014, Global Ozone Research and Monitoring Project – Report No. 55, 416 pp., Geneva, Switzerland, 2014.

**Table 1.** Overview over the chemistry-climate model simulations used for this analysis.

Types of Reference simulations (T42L90MA)	Hindcast 1980-2012 (nudged) RC1SD	Hindcast 1980-2012 (nudged) RC1SDNT	Hindcast 1960-2011 (free-running) RC1	Hindcast+future projection 1960-2040 (RCP6.0) (free-running) RC2
SST	ERA-interim	ERA-interim	HadSST/SSI	HadGEM simulated
Nudged QBO	+	+	+	+
Nudging of: vorticity, divergence, temperature, logarithm of surface pressure	+	+	-	-
Additional nudging of mean temperature	+	-	-	-

**Table 2.** Correlation of anomalies (de-trended, de-seasonalised) for RC1SD, RC1 and RC2 at 90 and 70 hPa, respectively.

Correlation of anomalies	1980–2012	1960–2011	1960–2030	1980–2012	1960–2011	1960–2030
	RC1SD	RC1	RC2	RC1SD	RC1	RC2
	70 hPa	70 hPa	70 hPa	90 hPa	90 hPa	90 hPa
Temperature-ozone	0.69	0.92	0.88	0.60	0.70	0.41
Temperature-upwelling	-0.70	-0.55	-0.44	-0.64	-0.61	-0.39
Temperature-QBO	0.42	0.52	0.47	0.25	-0.25	-0.12
Ozone-upwelling	-0.56	-0.62	-0.54	-0.54	-0.65	-0.45
Ozone-QBO	0.51	0.57	0.50	0.23	-0.38	-0.14
Temperature-moisture	0.37	0.84	0.80	0.86	0.94	0.90

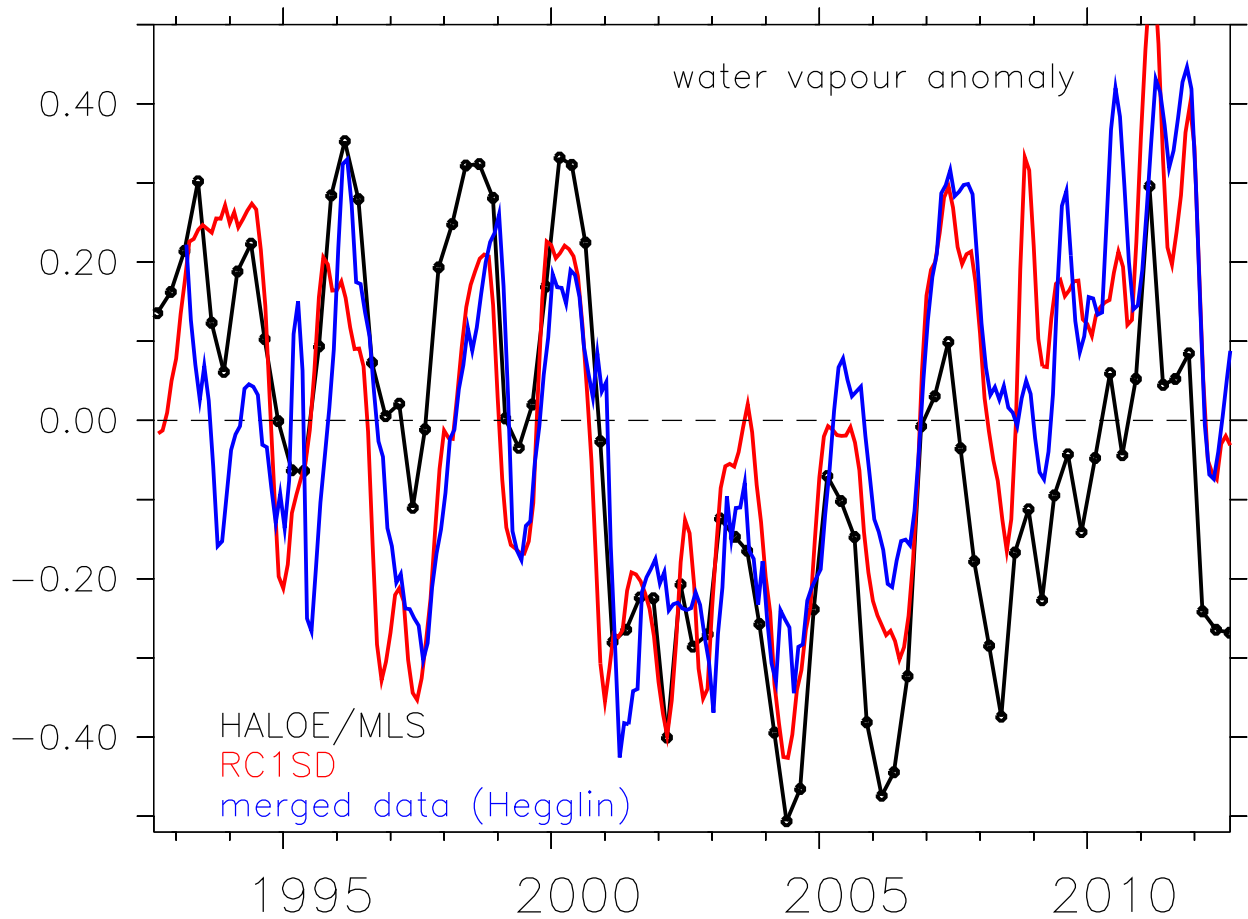


**Figure 1.** Interannual changes of the near-global mean ( $60^{\circ}$  S– $60^{\circ}$  N) stratospheric water vapour mixing ratios (in ppmv) at 83 hPa. The black line is the data derived from satellite observations (combined HALOE and Aura/MLS satellite measurements, de-seasonalised, 3 month average), which was published by Randel and Jensen (2013) in their Fig. 5a (upper graph). The red line is the RC1SD simulation (de-seasonalised, 3 month running mean). The blue line is the merged data set as published by (Hegglin et al., 2013). The correlation between HALOE/Aura/MLS and RC1SD is  $r=0.68$  and between the merged data set and RC1SD  $r=0.73$ . ( $r$ : Pearson’s correlation coefficient, see Appendix B).

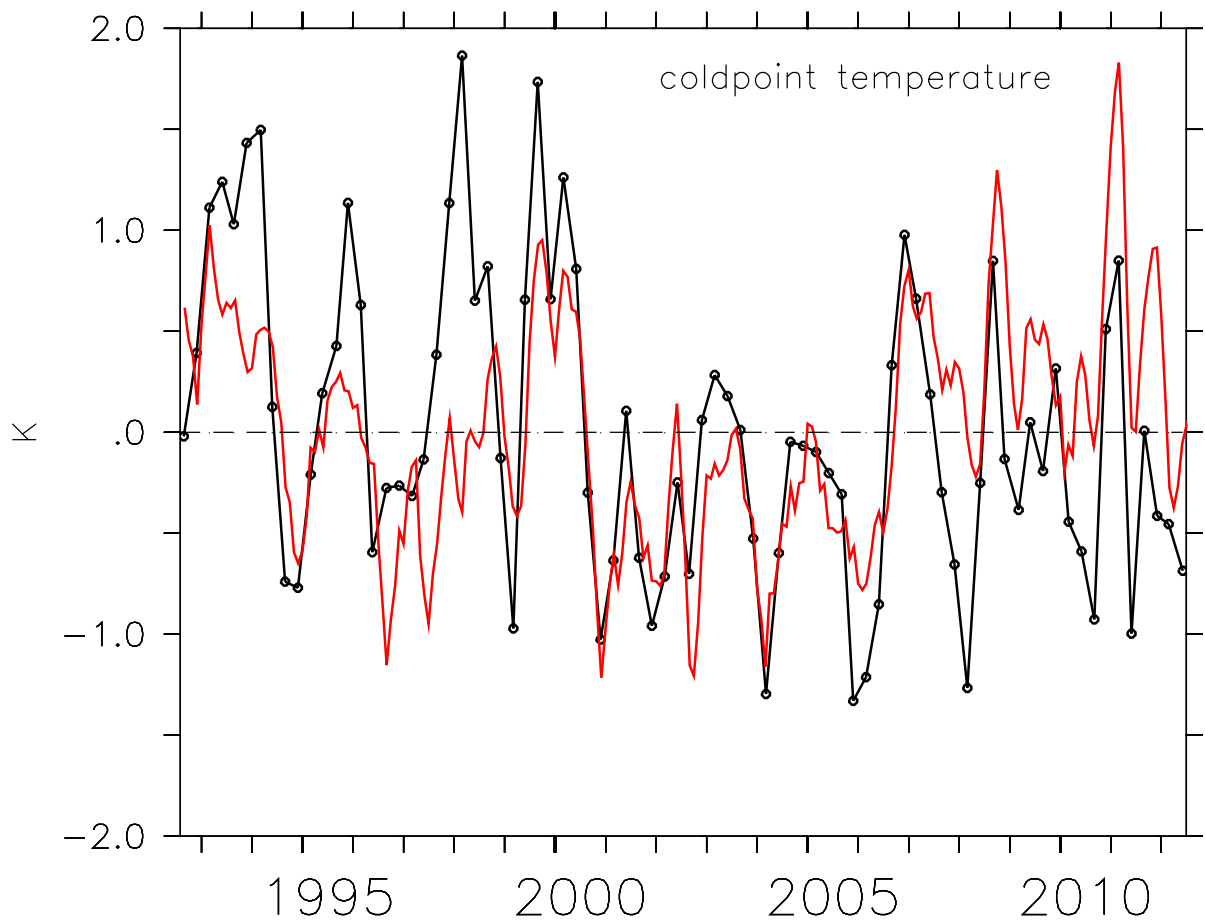


**Figure 2.** Cold point temperatures in the tropics ( $20^{\circ}$  S– $20^{\circ}$  N) derived from radiosonde data (black line). The data was already published by Randel and Jensen (2013) in their Fig. 5a (lower graph). The red line is the RC1SD simulation (de-seasonalised, 3 month running mean). The correlation coefficient is  $r=0.61$ .

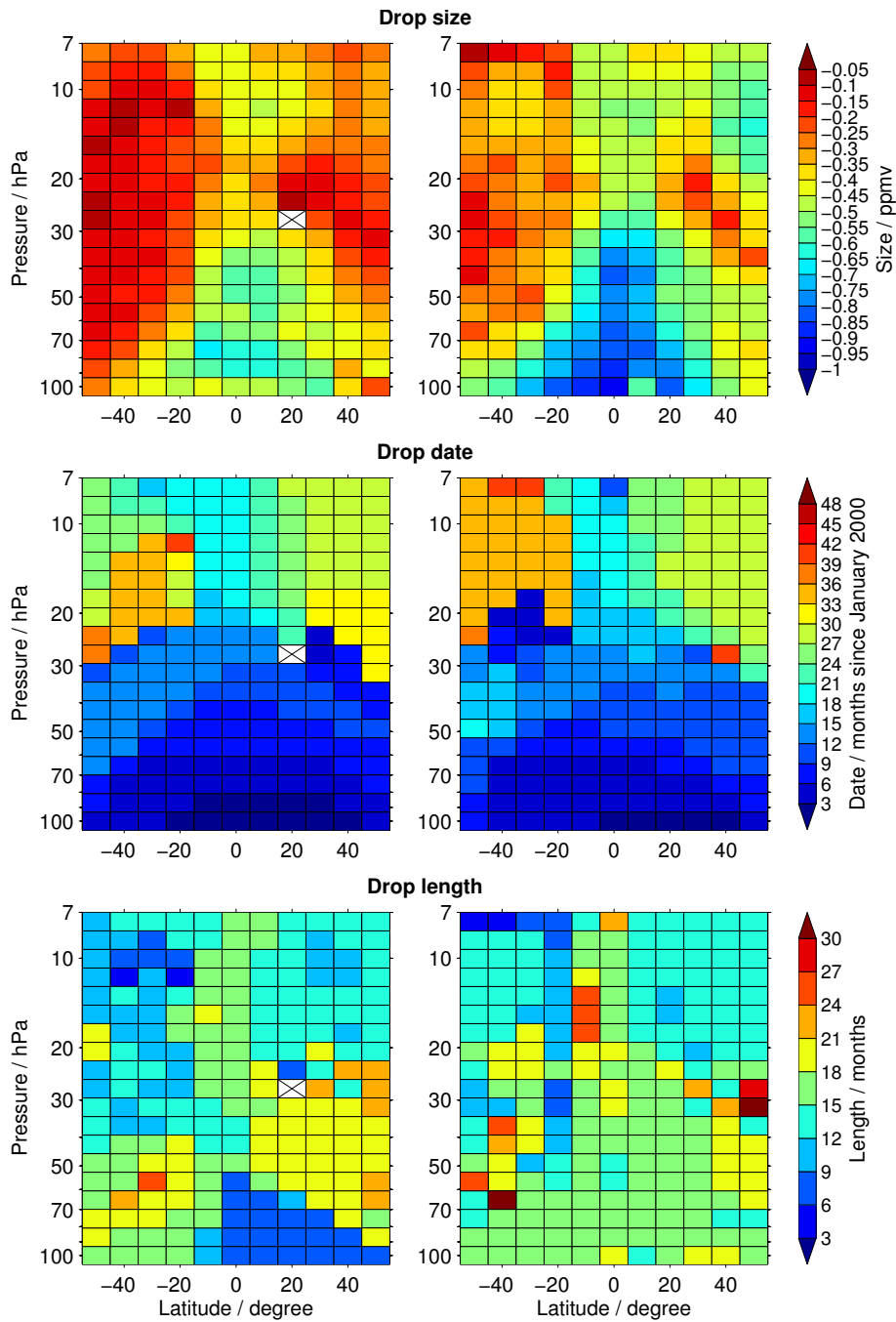


**Figure 3.** Characteristics of the millennium water vapour decline ([phase 1](#)) with respect to height (hPa). [The analysis approach of the water vapour decline is described in the Appendix A4.](#) RIGHT: Satellite observations. LEFT: RC1SD simulation. TOP: Drop size (amplitude)(unit: ppmv), MIDDLE: drop date (months since January 2000). BOTTOM: drop length (duration) (unit: months). White boxes with crosses indicate that the analysis failed to find a water vapour decrease that fulfilled the criteria listed in the Appendix A4.

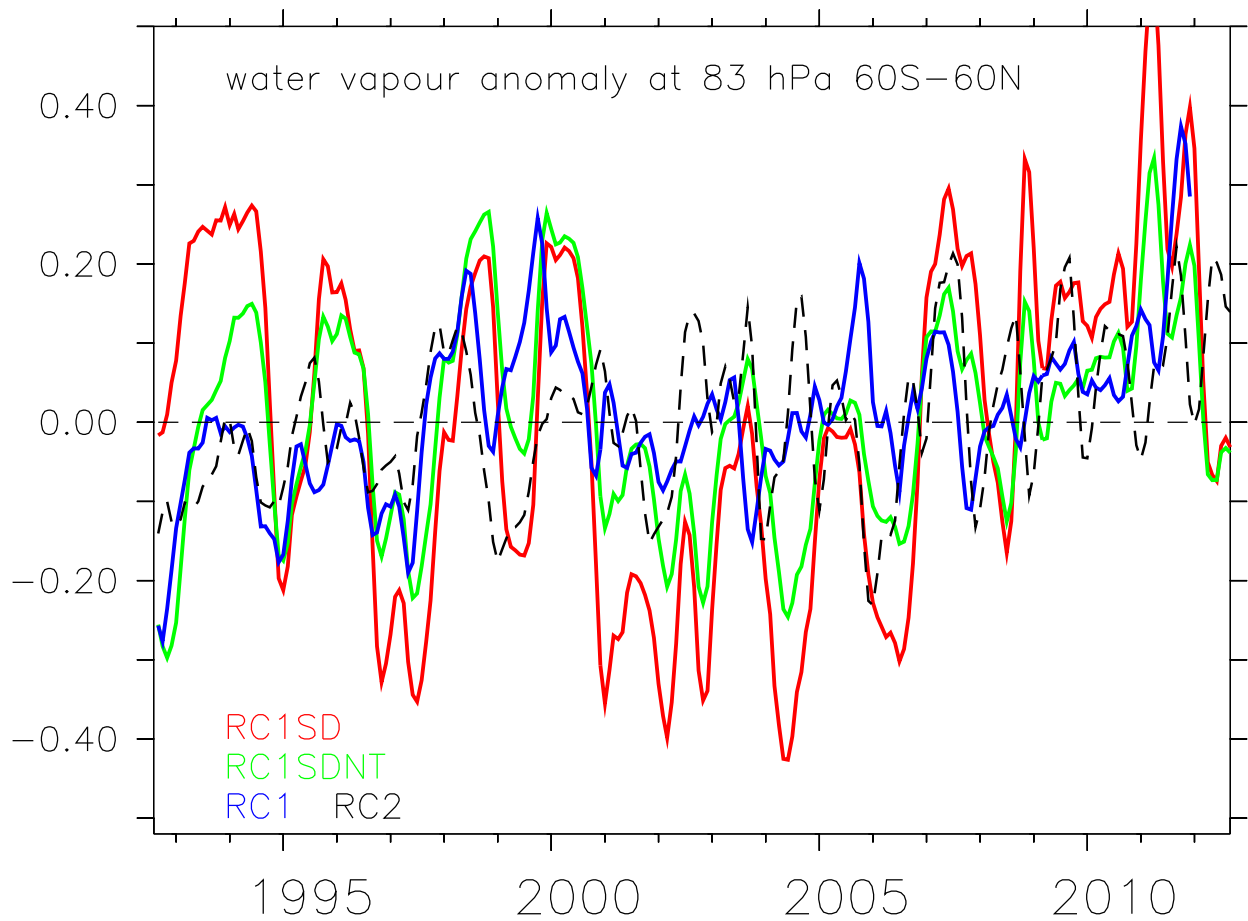


**Figure 4.** Near-global mean ( $60^{\circ}$  S– $60^{\circ}$  N) water vapour anomalies (de-seasonalised, note, these anomalies are a 12 month running mean and therefore slightly different compared to RC1SD in Fig. 1) derived from RC1SD, RC1SDNT, RC1 and RC2 simulations.



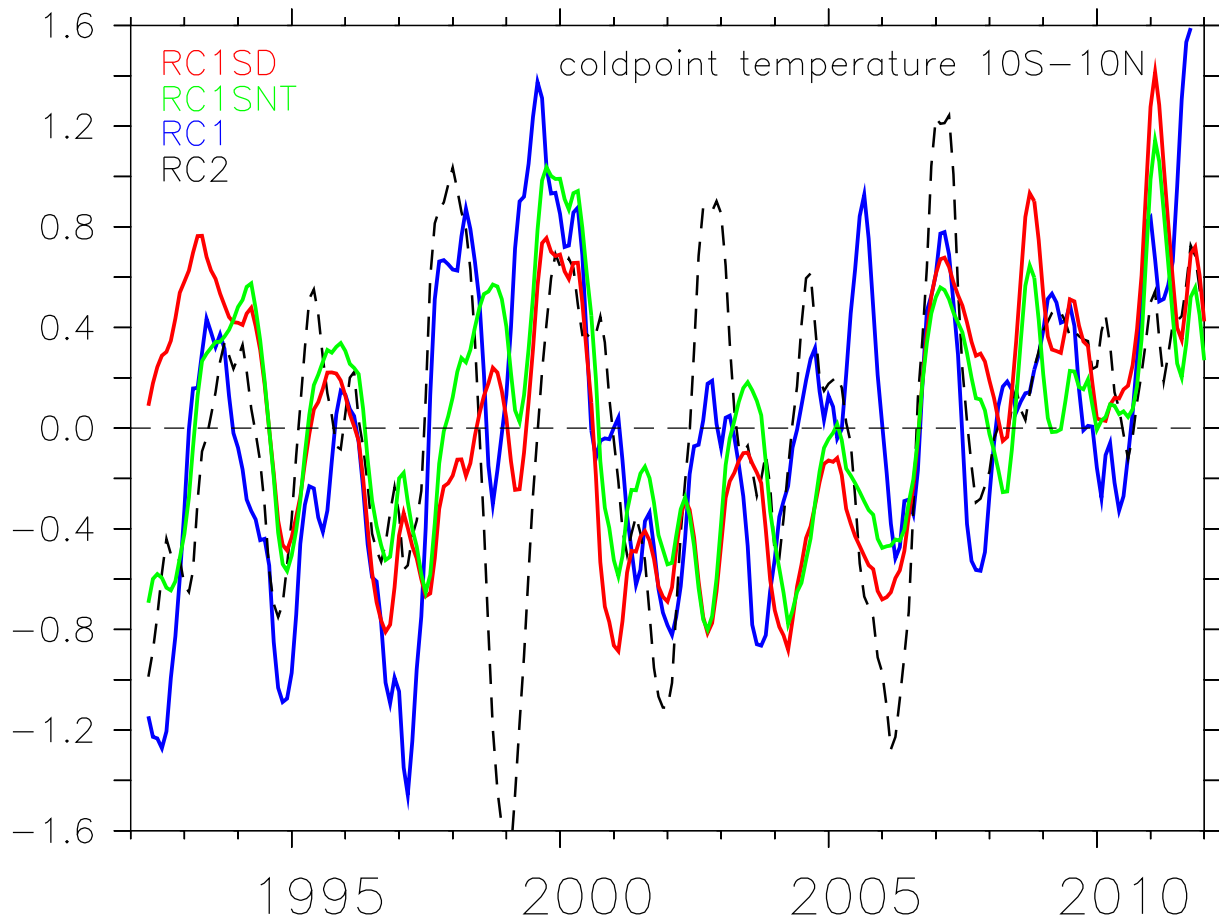


**Figure 5.** Cold point temperature anomalies (de-seasonalised, 12 month running mean) derived from RC1SD, RC1SDNT, RC1 and RC2 simulations.

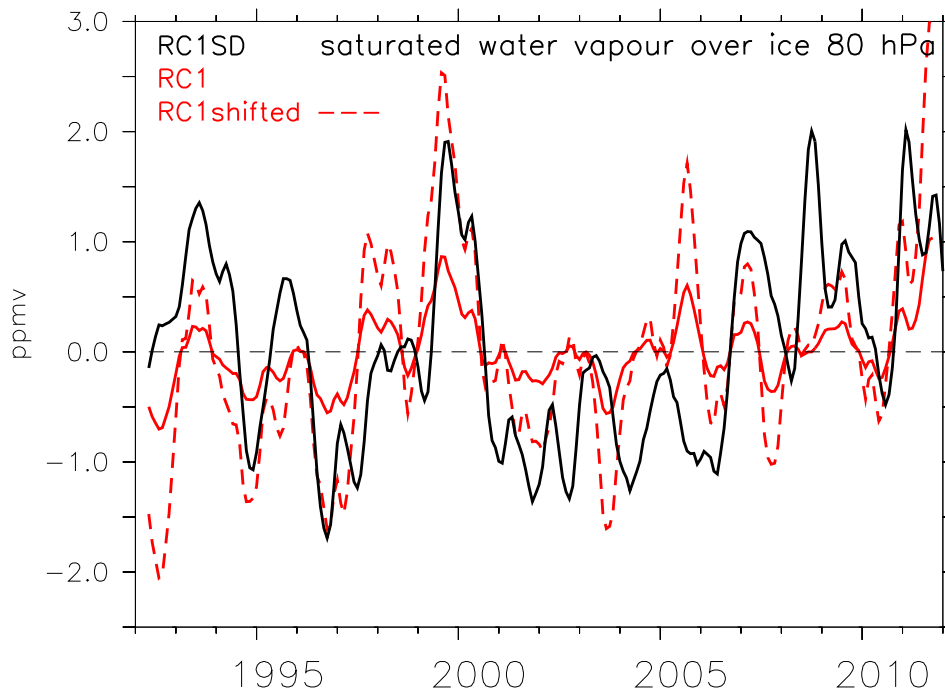


**Figure 6.** Saturation water vapour anomaly over ice (de-seasonalised, 6-month running mean) calculated from the respective cold point temperatures ( $10^{\circ}$  –  $10^{\circ}$  N) of RC1SD and RC1 simulations. RC1shift: mean cold point temperature of RC1 is shifted to RC1SD mean cold point temperature. The mean cold point temperatures are: RC1SD: 192.1 K, and RC1: 186.0 K, RC1shift: 192.1 K)

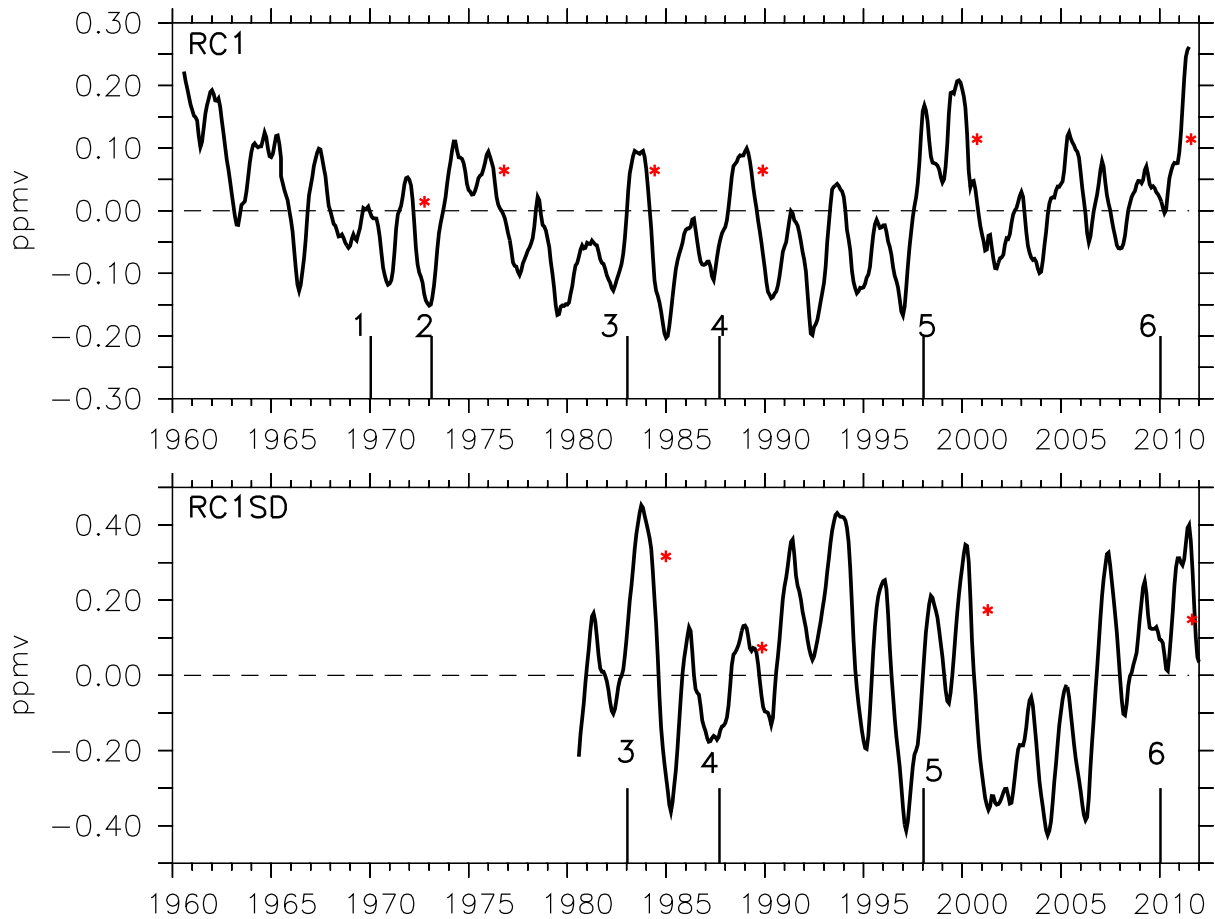


**Figure 7.** Moisture anomalies in ppmv (detrended, de-seasonalised, 12-months running mean) derived from RC1SD and RC1 simulations at 80 hPa. Black vertical lines mark [strong El Niño events](#) (see Fig. 8) and red asterisks mark the respective subsequent water vapour drop.

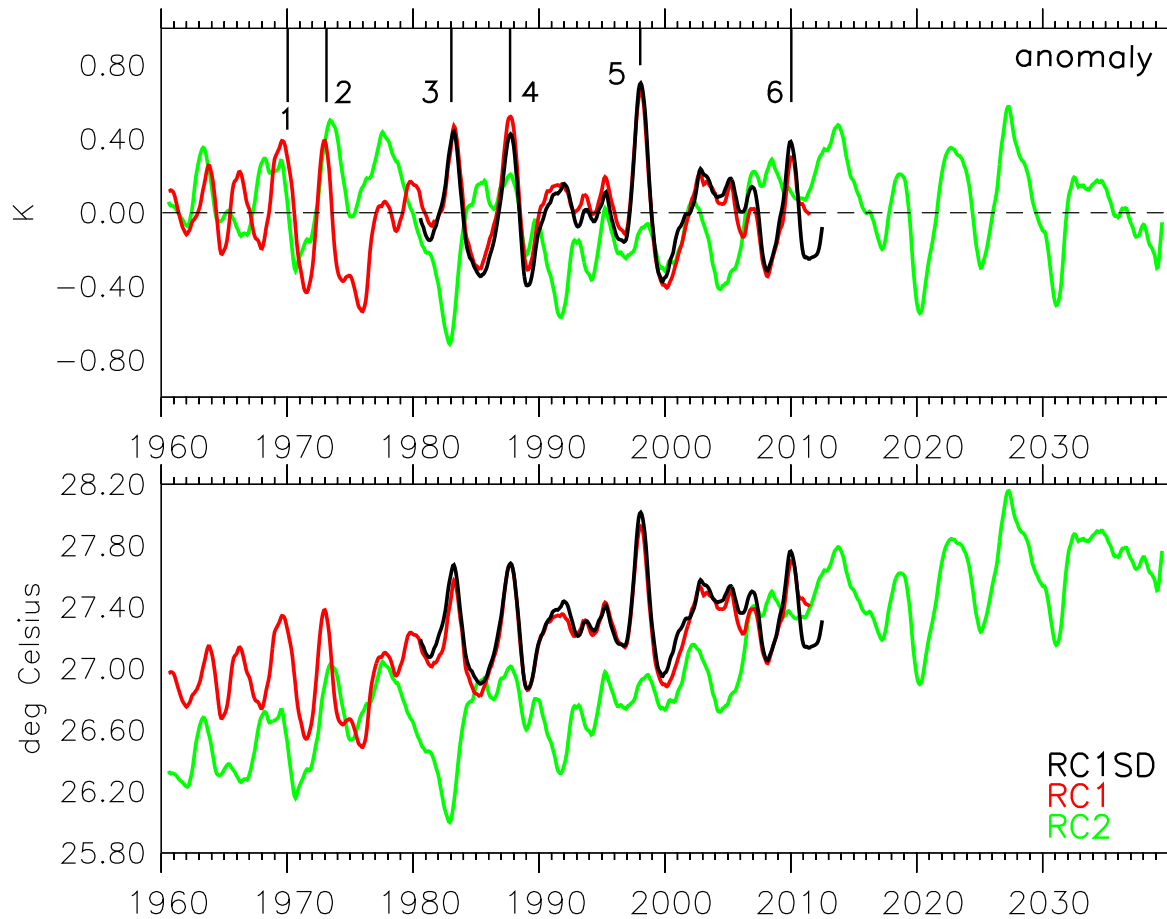


**Figure 8.** (a) Surface temperature anomaly in the tropical region ( $10^{\circ}\text{S}$ – $10^{\circ}\text{N}$ ) (de-trended, de-seasonalised, 12-point running mean) for RC1SD (black), RC1 (red) and RC2 (green). Strong El Niño/La-Niña events are labeled. (b) Surface temperature (degree Celsius) for RC1SD, RC1 and RC2 (12-point running mean).

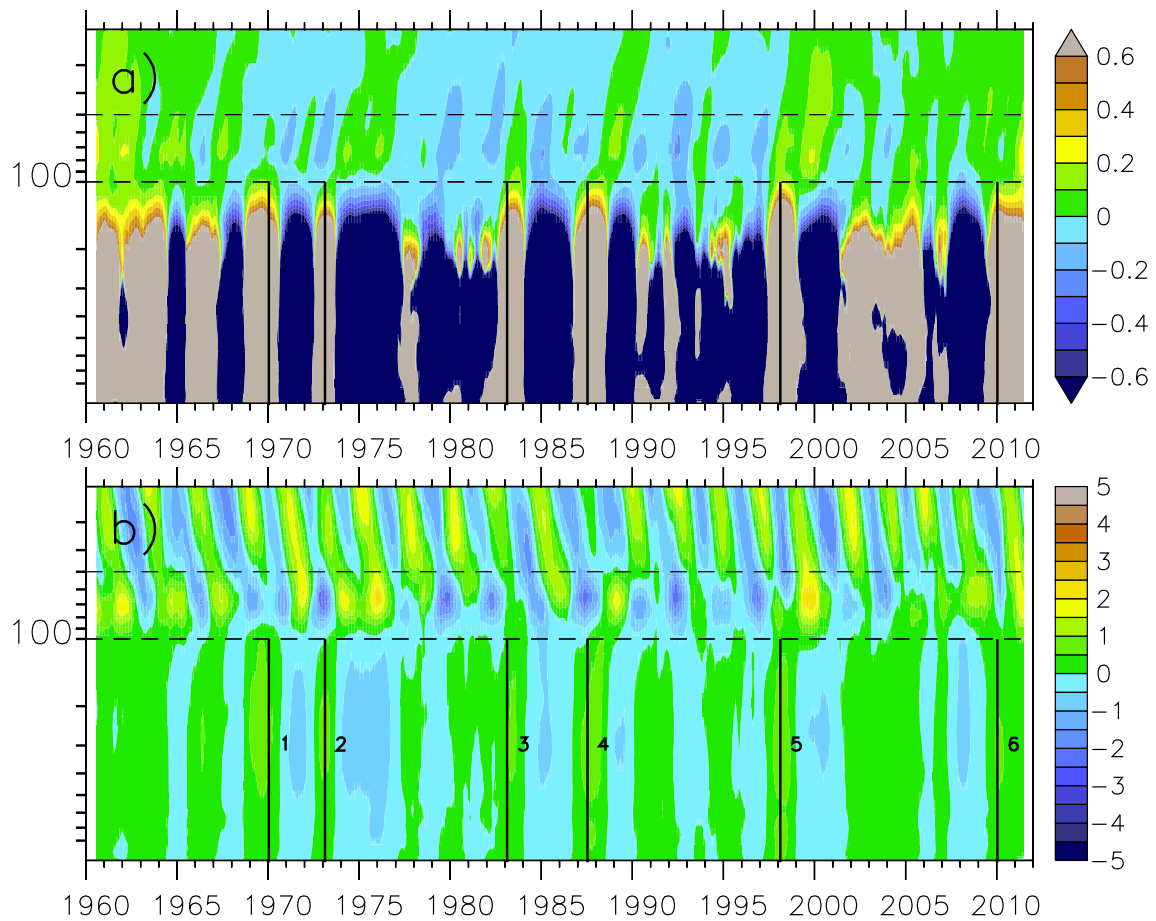


**Figure 9.** (a) Temporal evolution of moisture anomalies (ppmv). (b) Temporal evolution of temperature anomalies (K) in the tropical region (12 month running mean), derived from the RC1 simulation. Strong El Niño events are labelled [similar as in Fig. 8](#). The altitude range covers the pressure levels from 900 to 30 hPa. The dashed lines mark the region between 100 and 50 hPa.

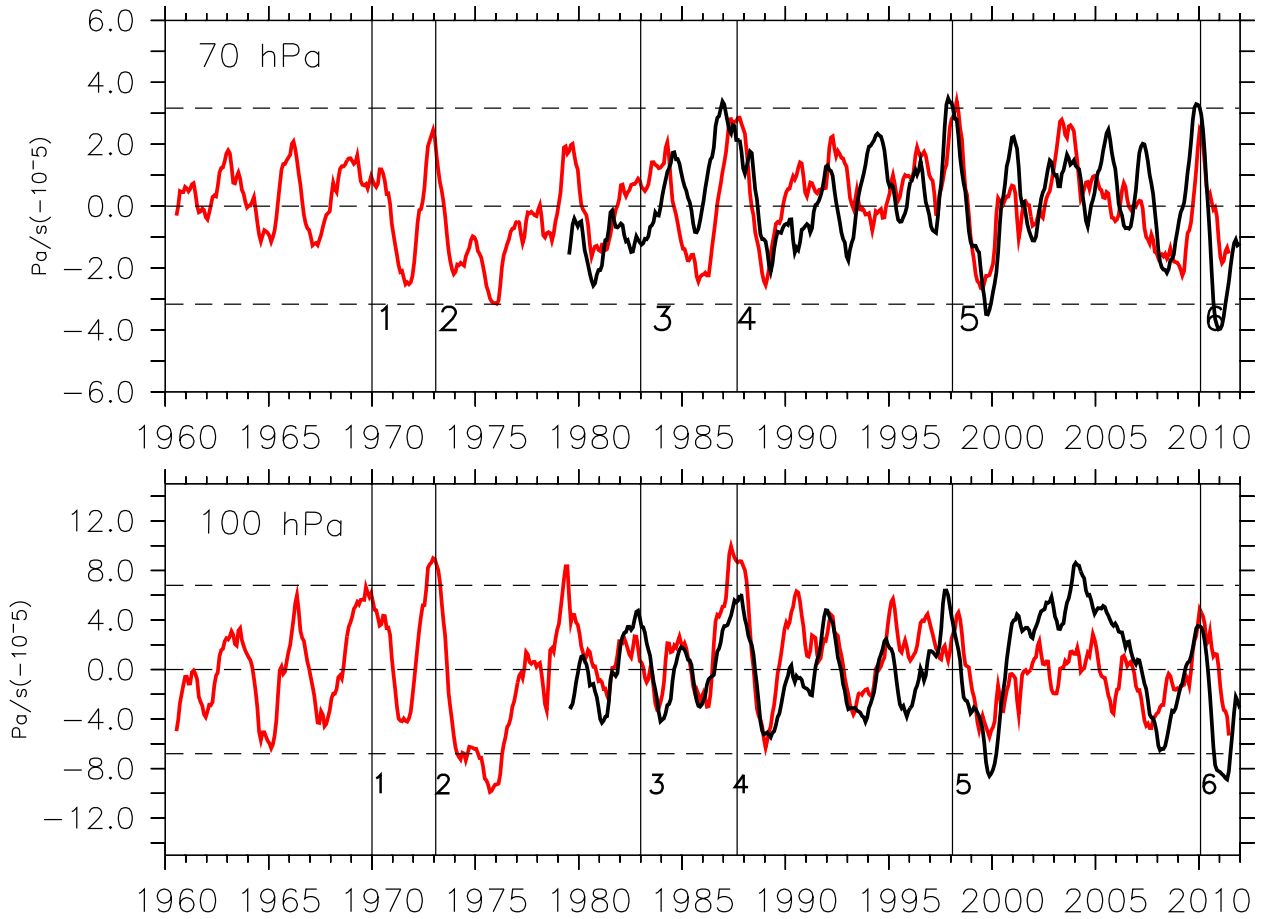


**Figure 10.** Temporal evolution of tropical upwelling anomalies in the tropics ( $20^{\circ}\text{S}$ – $20^{\circ}\text{N}$ ) (de-seasonalised and detrended) at 70 and 100 hPa (running mean). Red lines indicate data derived from RC1, black lines from RC1SD. Black dashed lines mark one standard deviation from the unsmoothed RC1SD monthly mean upwelling anomaly values. Black solid vertical lines mark El Niño events [similar as in Fig. 8.](#)

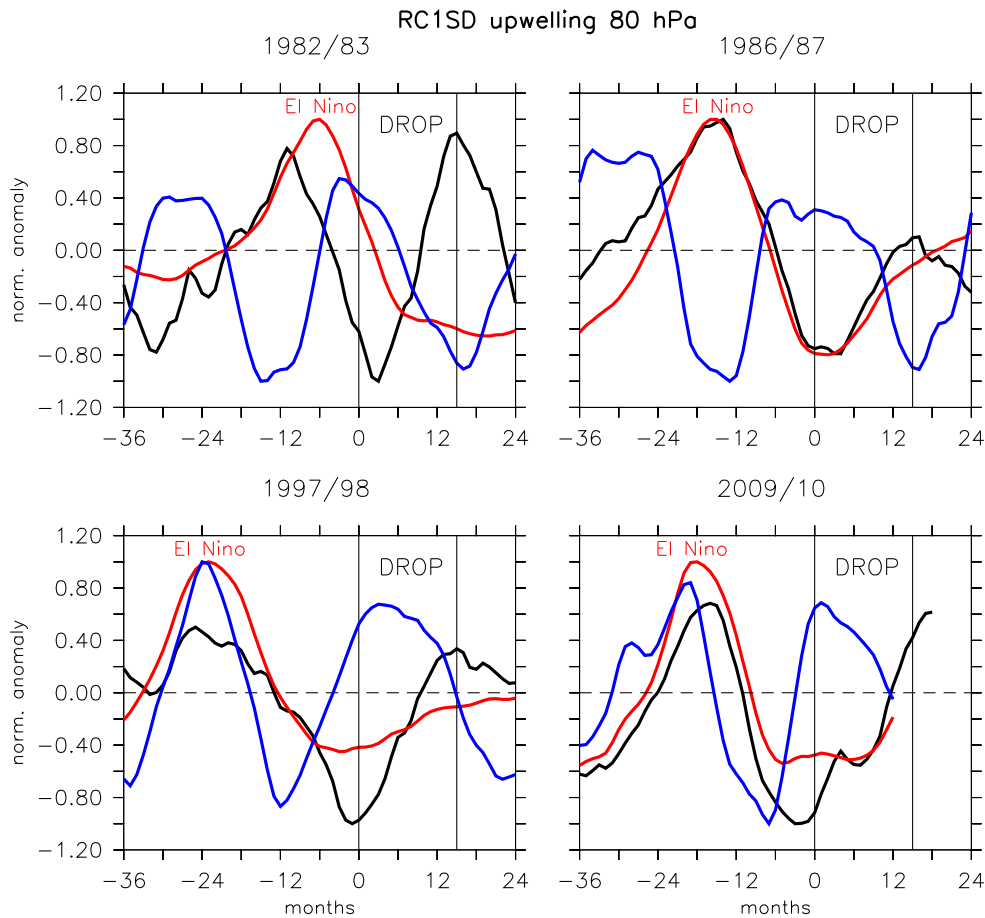


**Figure 11.** Episode analysis of for the zonal mean temperature-normalised upwelling anomaly at 80, tropical mean (black) for (10° S–10N–10° NS) at 80 hPa, de-seasonalized, de-trended, 12-point running mean, related to 4 different the max-normalised SST anomaly for the El Niño events in the RC1SD index 3.4 region (left red), and the RC1-max-normalised QBO (right blue) simulation for (10° N–10° S). The normalised upwelling anomaly is calculated by division of either the maximum or the absolute value of the minimum. For the SSTs and the QBO it is defined accordingly. Therefore, the results are dimensionless. All episodes are referenced to the beginning of the respective temperature drop. The drop onsets are accompanied by a negative upwelling anomaly.

Same as Fig. 11, but for the water vapour anomaly. Note that the vertical axis is smaller in the right figure.

Same as Fig. 11, but for tropical upwelling anomaly.

Same as Fig. 11, but for the ozone anomaly.

Same as Fig. 11, but for the QBO anomaly. The QBO is represented through the zonal wind anomaly.

Episode analysis for the normalised upwelling anomaly (black) for (10N–10S) at 80 hPa and the max-normalised SST anomaly for the El Niño index 3.4 region (red). The normalised upwelling anomaly is calculated by division of either the maximum or the absolute value of the minimum. For the SSTs it is defined accordingly. Therefore, the results are dimensionless. All episodes are referenced to the beginning of the temperature drop. The drop onsets are accompanied by a negative upwelling anomaly.

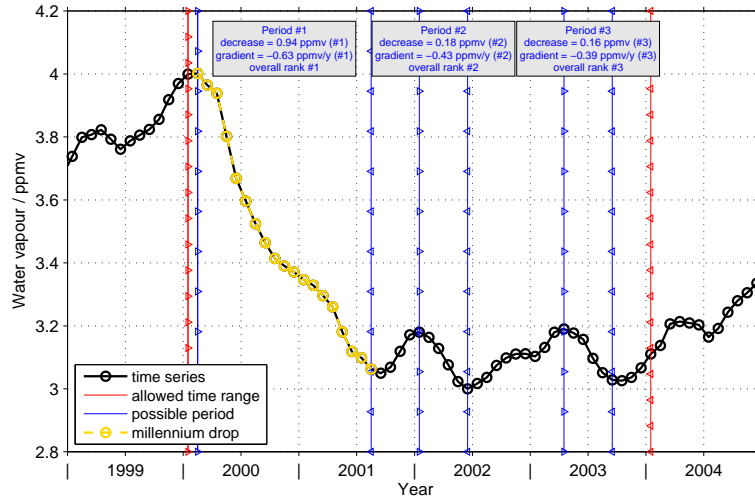


**Figure A1.** An example of the millennium drop (phase 1) characteristics analysis considering the HALOE/MIPAS time series at 100 hPa at the Equator. The time series is given in black and represents a running mean over one year. The red lines indicate the general time interval where a water vapour drop-decline will be considered. Within this period three periods can be found where water vapour is decreasing. The first period from February 2000 to August 2001 (overplotted in yellow) exhibits both the largest decrease and absolute gradient and is therefore selected as the representative period for the millennium drop (phase 1).

Episode analysis for the normalised upwelling anomaly at 80 hPa (black) for (10N-0S) and the max-normalised SST anomaly for the El Nio index 3.4 region (red). The normalised upwelling anomaly is calculated by division of either the maximum or the absolute value of the minimum. For the SSTs it is defined accordingly. Therefore, the results are dimensionless. All episodes are referenced to the beginning of the temperature drop. The drop onsets are accompanied by a negative upwelling anomaly.